# Taxonomy, genetic diversity, and phylogeny of the Antarctic mud dragon, Polacanthoderes (Kinorhyncha: Echinorhagata: Echinoderidae)

Yamasaki, Hiroshi
Faculty of Arts and Science, Kyushu University

Fujimoto, Shinta
Graduate School of Science and Technology for Innovation, Yamaguchi University

Tanaka, Hayato
Tokyo Sea Life Park

Shimada, Daisuke
Center for Molecular Biodiversity Research, National Museum of Nature and Science

他



出版情報：Zoologischer Anzeiger. 301, pp.42-58, 2022-11. Elsevier
バージョン：
権利関係：

# Taxonomy, genetic diversity, and phylogeny of the Antarctic mud dragon, *Polacanthoderes* (Kinorhyncha: Echinorhagata: Echinoderidae).

Hiroshi Yamasaki[1]*, Shinta Fujimoto[2], Hayato Tanaka[3], Daisuke Shimada[4], Masato Ito[5], Yuki Tokuda[6], Megumu Tsujimoto[5, 7]

1: Faculty of Arts and Science, Kyushu University, Fukuoka 819-0395, Japan
2: Graduate School of Science and Technology for Innovation, Yamaguchi University, 1677-1 Yoshida, Yamaguchi, Yamaguchi 753-8512, Japan
3: Tokyo Sea Life Park, 6-2-3 Rinkai-cho, Edogawa, Tokyo 134-8587, Japan
4: Center for Molecular Biodiversity Research, National Museum of Nature and Science, 4-4-1 Amakubo, Tsukuba, Ibaraki 305-0005, Japan
5: National Institute of Polar Research, 10-3 Midori-cho, Tachikawa, Tokyo 190-8518, Japan
6: Tottori University of Environmental Studies, 1-1-1 Wakabadaikita, Tottori 689-1111, Japan
7: Faculty of Environment and Information Studies, Keio University, 5322 Endo, Fujisawa, Kanagawa 252-0882, Japan

*Corresponding author. E-mail: h.yamasaki@meiobenthos.com

http://zoobank.org/XXXXXXXXXXXXXXXXXXXXXXXXXXXXXXXX
[The paper will be registered in Zoobank once it is accepted.]

## Abstract

A new species *Polacanthoderes shiraseae* sp. nov. from three Antarctic regions (off Cape Darnley, off Totten Glacier, and in Lützow-Holm Bay) is described. In addition, type species of *Polacanthoderes*, *Polacanthoderes martinezi*, is redescribed. The new species is distinguished from *P. martinezi* by the presence of conspicuously thick lateroventral acicular spines on segments 8 and 9 and the presence of sublateral small acicular spines on segment 7. Both *P. martinezi* and *P. shiraseae* sp. nov. occasionally show intraspecific morphological variations in the position of some small acicular spines. The K2P genetic distances based on the mitochondrial cytochrome *c* oxidase subunit 1 gene sequences in *P. shiraseae* sp. nov. are 0–1.5 %, equivalent to those in

other echinoderid species. Phylogenetic analyses of *Polacanthoderes* based on the nuclear 18S rRNA and 28S rRNA gene sequences support the inclusion of the genus in Echinorhagata/Echinoderidae and suggest that the genus represents the most basal group of this order/family.

**Keywords**

meiofauna, new species, K2P distance, JARE, DESS

## 1. Introduction

The family Echinoderidae includes five genera (*Cephalorhyncha* Adrianov, 1999 in Adrianov and Malakhov, 1999, *Echinoderes* Claparède, 1863, *Fissuroderes* Neuhaus and Blasche, 2006, *Meristoderes* Herranz et al., 2012, and *Polacanthoderes* Sørensen, 2008a) and ca. 160 species, representing the most species-rich taxon in Kinorhyncha (Adrianov and Maiorova, 2020; Cepeda et al., 2020; Grzelak et al., 2021; Rucci et al., 2022; Sørensen et al., 2015, 2020, 2021; Yamasaki et al., 2020a, b). Echinoderid species have been recorded worldwide, from tropical to polar areas and from various environments such as intertidal flats, sandy beaches, sandy/muddy shallow bottoms, deep-sea floors, seamounts, and submarine caves (e.g., Grzelak et al., 2021; Neuhaus, 2013; Sørensen et al., 2016; Yamasaki, 2016; Yamasaki et al., 2019; Yıldız et al., 2017). The recent phylogenetic, total-evidence, and phylogenomic analyses supported the family to solely represent the order Echinorhagata; Echinoderidae/Echinorhagata, Kentrorhagata, and Xenosomata comprise one of the two kinorhynch classes, Cyclorhagida, and within this class Echinoderidae/Echinorhagata is a sister taxon of Kentrorhagata; together these clades represent the sister group of Xenosomata (Dal Zotto et al., 2013; Herranz et al., 2022; Sørensen et al., 2015; Yamasaki et al., 2013). While the relationships of higher kinorhynch taxa were revealed recently, those of lower taxa (e.g., below the family level) are still unclear. This is partly because some genera and species are known only from remote environments, making it difficult to resample and obtain the molecular data for analysis.

*Polacanthoderes* is one of the groups known only from a remote environment, Antarctica. Although kinorhynch surveys have been conducted in many parts of the world in recent years (e.g., Cepeda et al., 2019; Dal Zotto and Todaro, 2016; Grzelak and Sørensen, 2019; Sánchez et al., 2012; Sørensen et al., 2012), *Polacanthoderes* species has never been recorded since Sørensen (2008a) reported the type species *Polacanthoderes martinezi* Sørensen, 2008a from the deep floor (2,274–2,290 m depth) offshore the South Shetland Islands. All the collected specimens of *P. martinezi* were formalin-fixed and provided a great deal of morphological data. Because of the presence of unique morphological traits, e.g., the presence of a large number of acicular spines on segments 4–10, *P. martinezi* was established as a new genus and species in Echinoderidae. However, due to the difficulty of recollecting *P. martinezi*, molecular data on the genus and species has not been available to date, and only morphological data has been used in subsequent phylogenetic analyses (Sørensen, 2008b; Sørensen et al., 2015).

Aside from the record of *P. martinezi*, there are only a very limited number of reports of Kinorhyncha from Antarctica, and most of them have been identified just as "Kinorhyncha sp." (e.g., Brannock et al., 2018; Ingels et al., 2006; Veit-Köhler et al., 2011). *Campyloderes vanhoeffeni* Zelinka, 1913 is the only kinorhynch identified to the species level other than *P. martinezi*. *Campyloderes vanhoeffeni* was first described based on the specimens collected at 385 m below the ice in the Antarctic Ocean during the Gauss expedition (the first German expedition to Antarctica): although the exact sampling coordinate is unknown, it is supposed to be around 66° S 90° E according to the shipping route record (Meinardus and Mecking, 1911; Zelinka, 1913). Subsequently, Neuhaus & Sørensen (2013) reported *Campyloderes* cf. *vanhoeffeni* at 411–801 m depth in the south of King George Island as well as at 2,893 m depth in the north of the South Shetland Islands. No kinorhynchs identified to the species level have been reported from Antarctica later on.

In this paper, we report a new species of *Polacanthoderes* from three regions in Antarctica collected during the 59th and the 61st Japanese Antarctic Research Expedition (JARE59 and JARE61, respectively). In addition to morphological data, we also succeeded in obtaining molecular data of several individuals of the new species. Using these data, the genetic diversity within the species as well as the phylogenetic position of *Polacanthoderes* within Kinorhyncha were investigated. We also report some morphological features of *P. martinezi* overlooked in the original description.

## 2. Material and methods

### 2.1. Sampling and morphological observation

During JARE59 and JARE61, sediment samples were obtained by a grab sampler at several stations off Cape Darnley, off Totten Glacier, and in Lützow-Holm Bay around Antarctica (Fig. 1; Table 1). Part of the sediment samples collected in JARE61 was fixed in 10% formalin immediately after sampling. The rest samples of JARE61 as well as all the samples of JARE59 have been kept frozen until the subsequent processing. In the laboratory, the samples were washed in a 32-μm sieve, and organisms were extracted from the sieved sediment using the floatation method with Ludox HS-40 (Giere, 2009; Higgins and Thiel, 1988). After sorting the extracted organisms under a stereomicroscope, kinorhynch specimens from the formalin-fixed sample were transferred to 70% EtOH, and those from the frozen sample were transferred to 99% EtOH or DESS solution (Yoder et al., 2006).

For light microscopic observation (LM), kinorhynch specimens were

transferred to dehydrated glycerine and individually mounted as glycerol-paraffin slides on Cobb aluminium frames or mounted in Fluoromount G® on H-S slides (Shirayama et al., 1993). Subsequently, they were observed with an Olympus BX53 microscope with differential interference contrast (DIC) and photographed with an Olympus DP74 camera. Measurements were made with Olympus cellSens software. A camera lucida equipped with the microscope was used to make drafts for line art illustrations. Final line illustrations were written out based on the drafts with Adobe Illustrator 2022.

Specimens for scanning electron microscopy (SEM) were transferred to dehydrate ethanol, immersed in 100% t-butyl alcohol, freeze-dried, mounted on aluminium stubs, sputter-coated with gold-palladium, and observed with a Hitachi SU3500 scanning electron microscope at Center for Advanced Instrumental and Educational Supports, Faculty of Agriculture, Kyushu University (Fukuoka, Japan).

The type specimens of *P. martinezi* for LM deposited at Museum für Naturkunde Berlin (Berlin, Germany), were observed with a Zeiss Axioskop 50 microscope equipped with a camera lucida. The line art illustrations were made with the same microscope by following the drawing method for the JARE specimens. Non-type specimens of *P. martinezi* for SEM, also deposited at the same museum were observed with a Zeiss EVO LS 10 scanning electron microscope. All observations of *P. martinezi* was done at the Museum für Naturkunde Berlin.

The type specimens of the JARE specimens have been deposited in the invertebrate collection of the Hokkaido University Museum, Hokkaido University, Sapporo, Japan (catalogue numbers ICHUM 8348–8404) and the Natural History Museum of Denmark, Copenhagen, Denmark (catalogue numbers NHMD 1174924–1174933).

The map was drawn with the Generic Mapping Tools (GMT) (Wessel et al., 2013), and subsequently modified with Adobe Illustrator 2022.

### 2.2. Molecular analyses

Total genomic DNA was extracted from 23 JARE specimens. Extractions were performed on single individuals with a DNeasy Tissue Kit (Qiagen, Tokyo), following the protocol of Yamasaki et al. (2013). After DNA extraction, the exoskeleton of each specimen was mounted for LM as described above. The exoskeletons of four specimens were lost during the DNA extraction. Parts of the nuclear 18S rRNA (18S) and 28S rRNA (28S) for a single individual, as well as a part of the mitochondrial cytochrome *c* oxidase subunit 1 (COI) for 21 individuals, were amplified by PCR with the primers

listed in Table 2. All nucleotide sequences were determined by direct sequencing with a BigDye Terminator Kit ver. 3.1 (Life Technologies, Co., USA) and a 3730 DNA Analyzer (Life Technologies, Co., USA). Sequence fragments were assembled by using MEGA X (Kumar et al., 2018). The assembled sequences were deposited in GenBank under accession numbers LC721243 (18S), LC721244 (28S), and LC721222–LC721242 (COI).

The COI sequences were used for calculating the intraspecific genetic variations by using MEGA X. After the alignment of the sequences, gap sites were completely removed, resulting in a 541 bp dataset. Subsequently, the Kimura (1980) 2-parameter (K2P) genetic distances among and within populations were calculated.

To detect the phylogenetic position of the genus *Polacanthoderes* within Kinorhyncha, a maximum likelihood (ML) analysis and Bayesian inference (BI) were conducted with the 18S and 28S sequences of kinorhynchs. The dataset was comprised of 20 out of the 31 kinorhynch genera (including four out of the five echinoderid genera) and two outgroup taxa (Priapulida and Nematoda) (Table 3). The remaining echinoderid genus, *Fissuroderes*, was not included in the dataset because sequence data of the genus has been unavailable so far. Sequences were aligned gene by gene using MAFFT software (Katoh and Toh, 2010). Ambiguous areas of alignments were removed using trimAl software (Capella-Gutiérrez et al., 2009). Gap sites were also removed except for the missing data regions. The resulting aligned sequences comprised 1353 bp (18S) and 2750 bp (28S). Homogeneity of base frequencies was tested gene by gene with a chi-square test in Kakusan4 (Tanabe, 2007), indicating $p > 0.05$ for each of 18S and 28S, i.e. the base composition was significantly homogeneous.

The ML analysis was constructed with RAxML-NG integrated in raxmlGUI 2.0 (Edler et al., 2021) and the BI analysis was conducted in MrBayes 3.2.7a (Huelsenbeck and Ronquist, 2001; Ronquist and Huelsenbeck, 2003; Ronquist et al., 2012). In both analyses, the data were partitioned by gene. The substitution models for each gene for ML were selected with raxmlGUI 2.0, and those for BI analyses were selected with Kakusan4. For ML trees, nodal support was assessed through analyses of 1000 bootstrap replicates. For BI, Markov-chain Monte-Carlo searches were performed with four chains, each of which was run for 1,000,000 generations, with trees sampled every 100 generations. Stationarity was evaluated by monitoring likelihood values graphically. The initial 10% of trees from each run were discarded as burn-in and the remaining trees were used to construct majority-rule consensus trees and determine the Bayesian posterior probability for each clade (Huelsenbeck and Ronquist 2001).

## 3. Results and Discussion

### 3.1. Taxonomy

**Class Cyclorhagida Zelinka, 1896 sensu Herranz et al. (2022)**
**Order Echinorhagata Sørensen et al., 2015**
**Family Echinoderidae Carus, 1885**
**Genus *Polacanthoderes* Sørensen, 2008a**

#### 3.1.1. Emended diagnosis for *Polacanthoderes*

Cuticle of first trunk segment forms complete ring; cuticle of segments 2–11 with midventral and lateroventral articulations resulting in one tergal and two sternal plates. Cuticular hairs and perforation sites absent on all segments. Primary pectinate fringe of ventral side on segment 1 with very large and conspicuous fringe tips; primary pectinate fringes of other areas on segment 1 and those on other segments with very small fringe tips. Middorsal acicular spines on segments 4–8; lateroventral acicular spines on segments 6–9; additional small acicular spines present in various positions on segments 4–10, at least in subdorsal position on segments 6 and 7, laterodorsal to midlateral position on segments 5–9, sublateral or lateral accessory position on segment 7, lateral accessory position on segments 6, 8, and 9, ventrolateral position on segments 8–10, and ventromedial position on segments 4–7. Tubes in midlateral position on segment 4; lateroventral position on segment 5; laterodorsal position on segment 10. Ventromedial setae present on segment 11. Females with ventromedial papillae on segment 6 and ventrolateral papillae on segment 7.

#### 3.1.2. *Polacanthoderes martinezi* Sørensen, 2008a

(Figs. 2–4; Table 4)

*Polacanthoderes martinezi* Sørensen 2008a: 230e3–230e11, figs 1–5, tables 1 and 2.

##### 3.1.2.1. Emended Diagnosis

*Polacanthoderes* with small lateral accessory acicular spines on segment 7; lateroventral acicular spines on segments 8 and 9 similar in width to those on segments 6 and 7.

### 3.1.2.2. Material examined

Holotype: Adult female, collected 14 February 2002 at north of South Shetland Islands (61°23.73′S, 58°50.26′W, 2274 m depth), mounted in Fluoromount G® (ZMB 11237). Allotype: Adult male, collected 14 February 2002 at north of South Shetland Islands (61°24.14′S, 58°51.15′W, 2290 m depth), mounted in Fluoromount G® (ZMB 11238a). Paratypes: Three adult females and one adult male, collected at the same time as holotype or allotype, mounted in Fluoromount G® (ZMB 11238b–d and 11238f). Non-types: three females and one male, collected at the same localities, mounted on aluminium stubs for SEM.

### 3.1.2.3. Redescription and remarks

Adult with head, neck, and eleven trunk segments (Figs. 2A–D and 3A–F). See table 1 in Sørensen (2008a) for measurements. Cuticular structures are summarized in Table 4. The distribution of cuticular structures generally follows the original description in Sørensen (2008a) (Figs. 2A–D, 3A–F, 4A–D), hence the following notes provide additional morphological data not mentioned in the original description.

Our observation confirmed the presence of all sensory spots and glandular cell outlets mentioned in Sørensen (2008a). In addition to the original description, the following previously unnoticed features were observed: the presence of subdorsal and laterodorsal sensory spots as well as ventromedial type-1 glandular cell outlets on segment 1 (Figs. 2A, B, and 3A–C); ventromedial sensory spots and middorsal type-1 glandular cell outlet on segment 2 (Fig. 2A, B); ventromedial sensory spots on segments 3 and 4 (Figs. 2B and 4A); paradorsal sensory spots on segments 6–8 (Fig. 2A); two pairs of subdorsal sensory spots on segment 9 (Figs. 2A and 3D); and subdorsal sensory spots on segments 10 and 11 (Figs. 2A, C, 3D). Segment 9 also possesses small-rounded sieve plates in the sublateral position (Fig. 2A, B). Females with ventromedial papillae on segment 6 and ventrolateral papillae on segment 7 (Figs. 2B, 3E, and 4C, D compared to Fig. 3F). We also confirmed the presence of long setae on segment 11 in both females and males (Fig. 2A–D).

Among the tubes and acicular spines on the trunk segments, the midlateral ones on segment 4 were referred to as “spines” in the original description. However, our observation confirmed they are thinner than the following small acicular spines and most likely not spines but tubes (Figs. 2A, 3C, 4A). The original description also mentioned the variable occurrence of some spines on segments 8 and 9. We additionally found the presence of subdorsal tubes on segment 2 only in one specimen (ZMB 11238a) (Fig. 3C); subdorsal small acicular spines or tubes on segment 5 in two

specimens (ZMB 11238a and a male SEM specimen); and the absence of midlateral tubes on segment 4 in one specimen (ZMB 11238d).

### 3.1.3. *Polacanthoderes shiraseae* Yamasaki, sp. nov.

(Figs. 5–9; Tables 5 and 6)

#### 3.1.3.1. Diagnosis

*Polacanthoderes* with sublateral small acicular spines on segment 7; lateroventral acicular spines on segments 8 and 9 being conspicuously thicker than those on segments 6 and 7.

#### 3.1.3.2. Etymology

The specific name "*shiraseae*" is a noun in the genitive case, named after the Japanese icebreaker *Shirase*, which was used for collecting the sediment sample containing *P. shiraseae* sp. nov.

#### 3.1.3.3. Material examined

Holotype: Adult female (catalogue No. ICHUM 8348), collected 19 December 2019 from off Totten Glacier, Antarctica (66°47′31"S, 117°21′20"E, 691 m depth), mounted in Fluoromount G® on H-S slides. Paratypes: 30 adult males and 36 adult females (catalogue no. ICHUM 8349–8404 and NHMD 1174924–1174933), detailed sampling data shown in the table 1, all individually mounted in Fluoromount G® on H-S slides. Non-type: nine adult males and eight adult females, detailed sampling data shown in the table 1, mounted on aluminium stubs for SEM.

#### 3.1.3.4. Type locality

Off Totten Glacier, Antarctica (66°47′31.20"S, 117°21′19.80"E), 691 m depth.

#### 3.1.3.5. Description

Adult with head, neck, and eleven trunk segments (Figs. 5, 6A–D, and 7A). See Table 5 for measurements. Table 6 indicates the positions of cuticular structures.

Head consists of retractable mouth cone and introvert (Fig. 7B). Distal part of mouth cone with pharynx crown, three rings of inner oral styles, and one ring of nine outer oral styles. Each of ring-03 and ring-02 bears five inner oral styles, whereas details of inner oral styles in ring-01 not observable. Outer oral styles alternating in

length: slightly longer in odd sectors than in even sectors. Outer oral style in sector 6 missing. Introvert with seven rings of spinoscalids and one ring of trichoscalids. Ring 01 with ten primary spinoscalids composed of one basal sheath and one distal end piece. Each basal sheath with two overlapping fringes: proximal fringe composed of several short projections between two long and slightly thicker lateral ones; distal fringe with several long projections. Distal end pieces of primary spinoscalids longest within all spinoscalids. Rings 02 and 04 with 10 spinoscalids; rings 03 and 05 with 20 spinoscalids. Each spinoscalid of rings 02–05 with basal sheath and end piece. Rings 06 and 07 not examined in detail, but with at least seven and four spinoscalids, respectively. Six trichoscalids covered with long hairs on entire surface and each attached to trichoscalid plates. Number and arrangement of inner oral styles, outer oral styles, and spinoscalids summarized in Fig. 8.

Neck with 16 placids (Figs. 5A, B, 6A, B, and 8). Midventral placid wider than others, and others similar in width.

Trunk with eleven segments; segment 1 consists of complete cuticular ring; segments 2–11 consist of one tergal and two sternal plates (Figs. 5 and 6A–D). Thickened cuticle forms pachycyclus at anterior margin and along midventral and tergosternal articulations of segments 2–10 (Fig. 6). Cuticular hairs and perforation sites absent on all segments (Figs. 6, 7, and 9).

Segment 1 (Figs. 5A, B, 6A, B, and 7C, D) with type-1 glandular cell outlet in middorsal position. Additional pair of type-1 glandular cell outlets in ventromedial position. Sensory spots present subdorsally, laterodorsally, sublaterally, and ventromedially. Posterior edge of this and following nine segments with primary pectinate fringe. Fringe tips of primary pectinate fringe in ventromedial area on segment 1 conspicuously large, whereas those in other areas and on other segments small and recognizable only in SEM.

Segment 2 (Figs. 5A, B, 6A, B, and 7C, D) with type-1 glandular cell outlets in middorsal and ventromedial positions. Two pairs of sensory spots present laterodorsally. Additional sensory spots present middorsally and ventromedially.

Segment 3 (Figs. 5A, B, 6A, B, and 7C, D) with middorsal and ventromedial type-1 glandular cell outlets. Sensory spots present in subdorsal, laterodorsal, midlateral, and ventromedial positions.

Segment 4 (Figs. 5A, B, 6A, B, and 7C–F) with middorsal acicular spine. Small acicular spines present ventromedially and tubes present midlaterally. Nineteen out of 84 examined specimens showed irregular spine patterns on this segment: 17 specimens with additional pair of subdorsal small acicular spines (e.g., compare Fig. 7E

and Fig. 7F); one specimen with additional midlateral small acicular spine/tube only on left side; one specimen lacks midlateral tubes. Type-1 glandular cell outlets present in paradorsal and ventromedial positions. Sensory spots present subdorsally and ventromedially.

Segment 5 (Figs. 5A, B, 6A, B, 7D–F, and 9A) with middorsal acicular spine. Small acicular spines present in midlateral and ventromedial positions, and tubes present in lateroventral position. Twenty-four out of 84 examined specimens showed irregular spine patterns on this segment: 23 specimens possess additional pair of subdorsal small acicular spines (e.g., compare Fig. 7E and Fig. 7F); one specimen with an additional subdorsal small acicular spine only on left side. Type-1 glandular cell outlets present in paradorsal and ventromedial positions. Sensory spots present subdorsally, midlaterally, and ventromedially.

Segment 6 (Figs. 5A, B, 6A, B, E–G, 7E, F, and 9A, B) with middorsal and lateroventral acicular spines. Small acicular spines present in subdorsal, laterodorsal, lateral accessory, and ventromedial positions. Three out of 84 examined specimens showed irregular spine patterns on this segment: lateral accessory small acicular spines moved to sublateral position in 2 specimens; one specimen with an additional sublateral small acicular spine only on right side. Type-1 glandular cell outlets present in paradorsal and ventromedial positions. Type-2 glandular cell outlets present in midlateral position. Sensory spots present paradorsal, subdorsal, and ventromedial positions. Ventromedial papillae present in females.

Segment 7 (Figs. 5A, B, 6C–G, 7A, E, and 9A–C) with middorsal and lateroventral acicular spines. Small acicular spines present subdorsally, laterodorsally, sublaterally, and ventromedially. Eight out of 84 examined specimens showed irregular spine pattern on this segment: sublateral small acicular spines moved to lateral accessory position in four specimens, of which one specimen also lacks lateroventral acicular spine on left side; one specimen with a non-paired sublateral small acicular spines on right side and paired lateral accessory small acicular spines; one specimen lacks one laterodorsal small acicular spine on right side; two specimens with one additional lateral accessory small acicular spines only on one side. Type-1 glandular cell outlets present in paradorsal and ventromedial positions. Sensory spots present paradorsally, subdorsally, midlaterally, and ventromedially. Papillae present in ventrolateral position in females.

Segment 8 (Figs. 5A, B, 6C, D, G, 7A, and 9B, C, E) with middorsal and lateroventral acicular spines. Lateroventral acicular spines conspicuously thicker and longer than those on previous two segments. Small acicular spines present laterodorsal,

lateral accessory, and ventrolateral positions. One out of 84 examined specimens with one subdorsal small acicular spine only on right side. Type-1 glandular cell outlets present paradorsally and ventromedially. Type-2 glandular cell outlets present in midlateral position. Sensory spots present in paradorsal, subdorsal, midlateral, and ventrolateral positions.

Segment 9 (Figs. 5A, B, 6C, D, and 9C–F) with lateroventral acicular spines, which are thicker than those on segments 6 and 7, but slightly shorter than those on segment 8. Small acicular spines present in laterodorsal, lateral accessory, and ventrolateral positions. Type-1 glandular cell outlets present paradorsally and ventromedially. Two pairs of sensory spots present in subdorsal position, and pair of sensory spots present in laterodorsal and ventrolateral positions. Small rounded sieve plate present sublaterally.

Segment 10 (Figs. 5, 6C, D, and 9E, F) with laterodorsal tubes and ventrolateral small acicular spines. Two type-1 glandular cell outlets present in middorsal position, and one pair in ventromedial position. Sensory spots present subdorsally and ventrolaterally.

Segment 11 (Figs. 5, 6C, D, H, and 9E, F) with lateral terminal spines. Males with three pairs of penile spines: most dorsal and most ventral penile spines quite slender and long, whereas middle penile spines much thicker and short. Females with lateral terminal accessory spines. Two type-1 glandular cell outlets present middorsally, and sensory spots present subdorsally. Surface of ventromedial area of sternal plates furry. Sternal plates triangle. Posterior edge of tergal plate protruding subdorsally forming pointed tergal extensions. Thin and long setae present next to tergal extensions in both males and females.

**3.1.3.6. Remarks**

*Polacanthoderes shiraseae* sp. nov. is similar to *P. martinezi* in many characters: the presence of (1) very strong and conspicuous pectinate fringe in the ventral side on segment 1, (2) middorsal acicular spines on segments 4–8, (3) lateroventral acicular spines on segments 6–9, (4) small acicular spines present at least in subdorsal on segments 6 and 7, laterodorsal on segments 5–9, lateral accessory on segments 6, 8, and 9, ventrolateral on segments 8–10, and ventromedial on segments 4–7, (5) tubes in midlateral on segment 4, lateroventral on segment 5, and laterodorsal on segment 10, (6) type-1 glandular cell outlets in middorsal on segments 1–3, 10, and 11, paradorsal on segments 4–9, ventromedial on segments 1–10, (7) type-2 glandular

cell outlets in midlateral on segments 6 and 8, and (8) ventromedial setae on segment 11, and (9) females with ventromedial papillae on segment 6 and ventrolateral papillae on segment 7 (Sørensen et al. 2008a). Furthermore, both of the two species sometimes possess irregular small acicular spines, especially on segments 4–8.

Although the two *Polacanthoderes* species share many characters, they can be distinguished clearly in the shapes of lateroventral acicular spines: the lateroventral acicular spines on segments 8 and 9 are conspicuously thicker than those on segments 6 and 7 in *P. shiraseae*, whereas those on segments 6–9 are all similar in width in *P. martinezi*. In addition, *P. shiraseae* can be distinguished from *P. martinezi* in the position of the small acicular spines on segment 7: the spines are in the sublateral position in the former, whereas they are in the lateral accessory position in the latter species. Although the spine position may be irregularly moved from sublateral to lateral accessory position in *P. shiraseae*, such a mutation seldom occurs (less than 10% of the examined specimens of *P. shiraseae* have small acicular spines in the lateral accessory position in segment 7). Furthermore, even if the spine position on segment 7 is inapplicable for some specimens, the width of the lateroventral acicular spines on segments 8 and 9 can be used for the identification of the species.

### 3.2. Genetic diversity within and among three populations of *Polacanthoderes*

The K2P genetic distances for the COI sequence showed distances within *P. shiraseae* are 0–1.5% (Table 7), which are comparable to the previously studied intraspecific K2P distances for other two echinoderid species (0–2.1% in *Echinoderes sensibilis*, 0–1.7% in *Echinoderes songae*) (Yamasaki et al., 2014). It should be noted that seven (six from off Cape Darnley and one from off Totten Glacier) out of the sequenced 21 individuals showed an irregular pattern in small acicular spines, but no great differences in K2P distances have not observed between them and "regular-spine pattern" individuals. Hence, the molecular data support such differences in the pattern of small acicular spines do not represent interspecific differences but intraspecific ones.

While the K2P values within and among the "off Totten Glacier" and "off Cape Darnley" populations are low (0–0.6%), those within the "Lützow-Holm Bay" as well as between "Lützow-Holm Bay" and the other two populations are relatively high (0.6–1.5%). This may suggest the presence of dispersal barrier(s) between Lützow-Holm Bay and Cape Darnley, and no barriers between Cape Darnley and Totten Glacier. Further studies with additional populations and study sites will provide more details on the mechanisms of the population connectivity of the species around

Antarctica.

### 3.3. Phylogenetic position of *Polacanthoderes*

The BI and ML analyses produced trees of very similar topology, hence we show the ML tree with nodal support (ML bootstrap values (BS) and BI posterior probability (PP)) in the Fig. 10. The resulted topology is mostly congruent with those of the previous phylogenetic and phylogenomic studies of kinorhynchs (Dal Zotto et al., 2013; Herranz et al., 2022; Sørensen et al., 2015; Yamasaki et al., 2013). The only remarkable difference among the new and previous results is the position of the clade *Paracentrophyes* + Franciscideridae (*Franciscideres* and *Gracilideres*): it is represented as the sister clade of Pycnophyidae in the analyses based on the 18S and 28S gene sequences (Yamasaki et al. 2013; Sørensen et al. 2015; this study), whereas it composes the Anomoirhaga clade together with *Dracoderes* and *Cateria* in the phylogenomic analyses (Herranz et al. 2022). Aside from the difference between this and previous analyses found in the Allomalorhagida clade, the relationships of cyclorhagids (Echinorhagata, Kentrorhagata, and Xenosomata) are consistent throughout all analyses.

In our results, the Echinorhagata/Echinoderidae clade including *Polacanthoderes*, *Cephalorhyncha*, *Echinoderes*, and *Meristoderes* was detected with high support values (nodal support bootstrap value/posterior probability = 100/1.00). In this clade, *Polacanthoderes* branches off most basally, representing the sister taxon to a clade with the remaining three genera. The clade *Cephalorhyncha* + *Echinoderes* + *Meristoderes* was also supported with high values (99/1.00), however, the monophyly of any of the three genera was not supported.

The phylogenetic position of *Polacanthoderes* detected by this study does not conflict with the previous analyses based on morphology (Sørensen, 2008b) or the total evidence analysis (Sørensen et al., 2015) but indicates its position more clearly. Both of the previous studies suggested the inclusion of *Polacanthoderes* in the family Echinoderidae, which is strongly supported by the current results. Sørensen (2008b) also suggested that *Polacanthoderes* is the most basal taxon of the family, being the sister taxon of the clade consisting of three echinoderid genera (*Cephalorhyncha*, *Echinoderes,* and *Fissuroderes*). In the total-evidence analysis in Sørensen et al. (2015), *Polacanthoderes* composed a clade together with *Fissuroderes*, but the root of the family appeared as an unresolved polytomy and failed to clarify the relationships between the *Polacanthoderes* + *Fissuroderes* clade and the remaining three echinoderid genera. Our new results support that *Polacanthoderes* is one of the most basal taxa of

Echinoderidae, and *Cephalorhyncha*, *Echinoderes*, and *Meristoderes* are more closely related to each other than to *Polacanthoderes.* Because our analyses lack *Fissuroderes* data, the phylogenetic position of *Fissuroderes* remains unclear. Nevertheless, considering the phylogenetic position of *Polacanthoderes*, there is no doubt that the genus is one of the key taxa to detect the evolution of Echinoderidae. Further analysis with broader taxon sampling, including *Fissuroderes* and various *Echinoderes* species, will provide a more detailed understanding of the phylogenetic relationships within the family Echinoderidae and their evolutionary history in the group.

## 4. Acknowledgments

We thank Dr Satoshi Imura and Dr Takeshi Tamura (National Institute of Polar Research, Research Organization of Information and Systems) and Dr Kay I Ohshima (Institute of Low Temperature Science, Hokkaido University) for their sincere support throughout this study; the officer, crew, and scientists on board the icebreaker *Shirase* for their assistance in the field operations and sample collections; Mr Koga Nakata (Kyushu University) and Mr Kaoru Kurosawa (Kyushu University) for their help in extracting meiofauna from the sediment samples; Dr Birger Neuhaus (Museum für Naturkunde Berlin, Germany) for his help in observing the type material of *Polacanthoderes martinezi*; Center for Advanced Instrumental and Educational Supports, Faculty of Agriculture (Kyushu University) for making facilities for SEM observation available. Sample collections during the JARE expeditions were supported by several KAKENHI Grants (17H01157, 17H01615, 17H04710, 17H06318, 17H06321, 18H01329, 18K13649, 19H00728, and 21H01201) from the Japan Society for the Promotion of Science, the Science Program of JARE as Prioritized Research Project (ROBOTICA), National Institute of Polar Research (NIPR) through Project Research KP-303 and KP-309, the Center for the Promotion of Integrated Sciences of SOKENDAI, and the Joint Research Program of the Institute of Low Temperature Science, Hokkaido University. After the sample collections, meiofaunal extraction, observation, and molecular work were carried out with a KAKENHI Grant (20H04974) to MT and another KAKENHI Grant (20K22670) to HY from the Japan Society for the Promotion of Science.

## References

Adrianov, A.V., Maiorova, A.S., 2020. *Echinoderes vulcanicus* sp. nov. from the active

marine volcano Piip – the first representative of the Kinorhyncha in the Bering Sea (Kinorhyncha: Cyclorhagida). Zool. Anz. 289, 35–49. https://doi.org/10.1016/j.jcz.2020.08.006

Adrianov, A.V., Malakhov, V.V., 1999. Cephalorhyncha of the World Ocean. KMK Scientific Press, Moscow.

Brannock, P.M., Learman, D.R., Mahon, A.R., Santos, S.R., Halanych, K.M., 2018. Meiobenthic community composition and biodiversity along a 5500 km transect of Western Antarctica: a metabarcoding analysis. Mar. Ecol. Prog. Ser. 603, 47–60. https://doi.org/10.3354/meps12717

Capella-Gutierrez, S., Silla-Martinez, J.M., Gabaldon, T., 2009. TrimAl: a tool for automated alignment trimming in large-scale phylogenetic analyses. Bioinform. 25, 1972–1973. https://doi.org/10.1093/bioinformatics/btp348

Carus, J.V., 1885. Prodromus Faunae Mediterraneae sive Descriptio Animalium Maris Mediterranei Incolarum quam Comparata Silva Rerum Quatenus Innotuit Adiectis Locis et Nominibus Vulgaribus Eorumque Auctoribus in Commodum Zoologorum, Vol. I, Coelenterata, Echinodermata, Vermes, Arthropoda. E. Schweizerbart'sche Verlagshandlung (E. Koch), Stuttgart.

Cepeda, D., Pardos, F., Zeppilli, D., Sánchez, N., 2020. Dragons of the deep sea: Kinorhyncha communities in a pockmark field at Mozambique Channel, with the description of three new species. Front. Mar. Sci. 7, 665. https://doi.org/10.3389/fmars.2020.00665

Cepeda, D., Sánchez, N., Pardos, F., 2019. First extensive account of the phylum Kinorhyncha from Haiti and the Dominican Republic (Caribbean Sea), with the description of four new species. Mar. Biodiv. 49, 2281–2309. https://doi.org/10.1007/s12526-019-00963-x

Claparède, R.E., 1863. Beobachtungen über Anatomie und Entwicklungsgeschichte wirbelloser Thiere an der Küste von Normandie angestellt. Verlag von Wilhelm Engelmann, Leipzig.

Dal Zotto, M., Di Domenico, M., Garraffoni, A., Sørensen, M.V., 2013. *Franciscideres* gen. nov. – a new, highly aberrant kinorhynch genus from Brazil, with an analysis of its phylogenetic position. Syst. Biodivers. 11, 303–321. https://doi.org/10.1080/14772000.2013.819045

Dal Zotto, M., Todaro, M.A., 2016. Kinorhyncha from Italy, a revision of the current checklist and an account of the recent investigations. Zool. Anz. 265, 90–107. https://doi.org/10.1016/j.jcz.2016.01.004

Edler, D., Klein, J., Antonelli, A., Silvestro, D., 2021. raxmlGUI 2.0: A graphical

interface and toolkit for phylogenetic analyses using RAxML. Methods Ecol. Evol. 12, 373–377. https://doi.org/10.1111/2041-210X.13512

Folmer, O., Black, M., Hoeh, W., Lutz, R., Vrijenhoek, R., 1994. DNA primers for amplification of mitochondrial cytochrome c oxidase subunit I from diverse metazoan invertebrates. Mol. Mar. Biol. Biotechnol. 3, 294–299

Giere, O., 2009. Meiobenthology. The microscopic motile fauna of aquatic sediments. Second Edition. Springer Verlag, Berlin.

Grzelak, K., Zeppilli, D., Shimabukuro, M., Sørensen, M.V., 2021. Hadal mud dragons: first insight into the diversity of Kinorhyncha from the Atacama Trench. Front. Mar. Sci. 8, 670735. https://doi.org/10.3389/fmars.2021.670735

Grzelak, K., Sørensen, M.V., 2019. Diversity and community structure of kinorhynchs around Svalbard: First insights into spatial patterns and environmental drivers. Zool. Anz. 282, 31–43. https://doi.org/10.1016/j.jcz.2019.05.009

Gutiérrez-Gutiérrez, C., Palomares Rius, J.E., Cantalapiedra-Navarrete, C., Landa, B.B., Castillo, P., 2011. Prevalence, polyphasic identification, and molecular phylogeny of dagger and needle nematodes infesting vineyards in southern Spain. Eur. J. Plant Pathol. 129, 427–453. https://doi.org/10.1007/s10658-010-9705-y

Herranz, M., Stiller, J., Worsaae, K., Sørensen, M.V., 2022. Phylogenomic analyses of mud dragons (Kinorhyncha). Mol. Phylogenet. Evol. 168, 107375. https://doi.org/10.1016/j.ympev.2021.107375

Herranz, M., Thormar, J., Benito, J., Sánchez, N., Pardos, F., 2012. *Meristoderes* gen. nov., a new kinorhynch genus, with the description of two new species and their implications for echinoderid phylogeny (Kinorhyncha: Cyclorhagida, Echinoderidae). Zool. Anz. 251, 161–179. https://doi.org/10.1016/j.jcz.2011.08.004

Higgins, R.P., Thiel, H., 1988. Introduction to the Study of Meiofauna. Smithsonian Institution Press, Washington DC.

Huelsenbeck, J.P., Ronquist, F., 2001. MRBAYES: Bayesian inference of phylogeny. Bioinform. 17, 754–755. https://doi.org/10.1093/bioinformatics/17.8.754

Ingels, J., Vanhove, S., De Mesel, I., Vanreusel, A., 2006. The biodiversity and biogeography of the free-living nematode genera *Desmodora* and *Desmodorella* (family Desmodoridae) at both sides of the Scotia Arc. Polar Biol. 29, 936–949. https://doi.org/10.1007/s00300-006-0135-4

Katoh, K., Toh, H., 2010. Parallelization of the MAFFT multiple sequence alignment program. Bioinform. 26, 1899–1900. https://doi.org/10.1093/bioinformatics/btq224

Kim, C.-G., Zhou, H.-Z., Imura, Y., Tominaga, O., Su, Z.-H., Osawa, S., 2000. Pattern of morphological diversification in the *Leptocarabus* ground beetles (Coleoptera: Carabidae) as deduced from mitochondrial ND5 gene and nuclear 28S rRNA sequences. Mol. Biol. Evol. 17, 137–145. https://doi.org/10.1093/oxfordjournals.molbev.a026226

Kimura, M., 1980. A simple method for estimating evolutionary rates of base substitutions through comparative studies of nucleotide sequences. J. Mol. Evol. 16, 111–120. https://doi.org/10.1007/BF01731581

Kumar, S., Stecher, G., Li, M., Knyaz, C., Tamura, K., 2018. MEGA X: Molecular Evolutionary Genetics Analysis across computing platforms. Mol. Biol. Evol. 35,1547–1549. https://doi.org/10.1093/molbev/msy096

Luan, Y., Mallatt, J.M., Xie, R., Yang, Y., Yin, W., 2005. The phylogenetic positions of three basal-hexapod groups (Protura, Diplura, and Collembola) based on ribosomal RNA gene sequences. Mol. Biol. Evol. 22, 1579–1592. https://doi.org/10.1093/molbev/msi148

Mallatt, J.M., Garey, J.R., Shultz, J.W., 2004. Ecdysozoan phylogeny and Bayesian inference: first use of nearly complete 28S and 18S rRNA gene sequences to classify the arthropods and their kin. Mol. Phylogenet. Evol. 31, 178–191. https://doi.org/10.1016/j.ympev.2003.07.013

Meinardus, W., Mecking, L., 1911. Meteorologischer Atlas, Deutsche Südpolar Expedition 1901-1903, Georg Reimer, Berlin.

Neuhaus, B., 2013. 5. Kinorhyncha (= Echinodera), in*:* Schmidt-Rhaesa, A. (Ed.), Handbook of Zoology. Gastrotricha, Cycloneuralia and Gnathifera. Volume 1: Nematomorpha, Priapulida, Kinorhyncha, Loricifera. Walter de Gruyter, Berlin, pp. 177–348.

Neuhaus, B., Blasche, T., 2006. *Fissuroderes*, a new genus of Kinorhyncha (Cyclorhagida) from the deep sea and continental shelf of New Zealand and from the continental shelf of Costa Rica. Zool. Anz. 245, 19–52. https://doi.org/10.1016/j.jcz.2006.03.003

Neuhaus, B., Sørensen, M.V., 2013. Populations of *Campyloderes* sp. (Kinorhyncha, Cyclorhagida): One global species with significant morphological variation? Zool. Anz. 252, 48–75. https://doi.org/10.1016/j.jcz.2012.03.002

Palumbi, S.R., 1996. Nucleic acids II: The polymerase chain reaction. In: Hills, D.M., Moritz, C., Mable, B.K. (Eds.), Molecular Systematics, Second Edition. Sinauer Associates, Sunderland, Massachusetts, pp. 205–247.

Randsø, P.V., Yamasaki, H., Bownes, S.J., Herranz, M., Di Domenico, M., Qii, G.B.,

Sørensen, M.V., 2019. Phylogeny of the *Echinoderes coulli*-group (Kinorhyncha: Cyclorhagida: Echinoderidae) – a cosmopolitan species group trapped in the intertidal. Invertebr. Syst. 33, 501–517. https://doi.org/10.1071/IS18069

Ronquist, F., Huelsenbeck, J.P., 2003. MrBayes 3: Bayesian phylogenetic inference under mixed models. Bioinform. 19, 1572–1574. https://doi.org/10.1093/bioinformatics/btg180

Ronquist, F., Teslenko, M., van der Mark, P., Ayres, D.L., Darling, A., Höhna, S., Larget, B., Liu, L., Suchard, M.A., Huelsenbeck, J.P., 2012. MrBayes 3.2: Efficient Bayesian phylogenetic inference and model choice across a large model space. Syst. Biol. 61, 539–542. https://doi.org/10.1093/sysbio/sys029

Rucci, K.A., Neuhaus, B., Bulnes, V.N., 2022. A new species of *Echinoderes* (Kinorhyncha: Cyclorhagida: Echinoderidae) from the Argentinean continental shelf with notes on its postembryonic development and on subcuticular morphological characters unreported for Kinorhyncha. Zootaxa 5099, 65–90. https://doi.org/10.11646/zootaxa.5099.1.3

Sánchez, N., Herranz, M., Benito, J., Pardos, F., 2012. Kinorhyncha from the Iberian Peninsula: new data from the first intensive sampling campaigns. Zootaxa 3402, 24–44. https://doi.org/10.11646/zootaxa.3402.1.2

Sánchez, N., Yamasaki, H., Pardos, F., Sørensen, M.V., Martínez, A., 2016. Morphology disentangles the systematics of a ubiquitous but elusive meiofaunal group (Kinorhyncha: Pycnophyidae). Cladistics 32, 479–505. https://doi.org/10.1111/cla.12143

Shirayama, Y., Kaku, T., Higgins, R.P., 1993. Double-sided microscopic observation of meiofauna using an HS-Slide. Benthos Res. 44, 41–44. https://doi.org/10.5179/benthos1990.1993.44_41

Sørensen, M.V., 2008a. A new kinorhynch genus from the Antarctic deep sea and a new species of *Cephalorhyncha* from Hawaii (Kinorhyncha: Cyclorhagida: Echinoderidae). Org. Divers. Evol. 8, 230e1–230e18. https://doi.org/10.1016/j.ode.2007.11.003

Sørensen, M.V., 2008b. Phylogenetic analysis of the Echinoderidae (Kinorhyncha: Cyclorhagida). Org. Divers. Evol. 8, 233–246. https://doi.org/10.1016/j.ode.2007.11.002

Sørensen, M.V., Dal Zotto, M., Rho, H.S., Herranz, M., Sánchez, N., Pardos, F., Yamasaki, H., 2015. Phylogeny of Kinorhyncha based on morphology and two molecular loci. PLoS ONE 10, e0133440.

https://doi.org/10.1371/journal.pone.0133440

Sørensen, M.V., Gąsiorowski, L., Randsø, P.V., Sánchez, N., Neves, R.C., 2016. First report of kinorhynchs from Singapore, with the description of three new species. Raffles Bull. Zool. 64, 3–27. http://doi.org/10.5281/zenodo.4502533

Sørensen, M.V., Goetz, F.E., Herranz, M., Chang, C.Y., Chatterjee, T., Durucan, F., Neves, R.C., Yildiz, N.Ö., Norenburg, J., Yamasaki, H., 2020. Description, redescription and revision of sixteen putatively closely related species of *Echinoderes* (Kinorhyncha: Cyclorhagida), with the proposition of a new species group – the *Echinoderes dujardinii* group. Eur. J. Taxon. 730, 1–101. https://doi.org/10.5852/ejt.2020.730.1197

Sørensen, M.V., Herranz, M., Pardos, F., Durucan, F., 2021. Kinorhynchs from sandy coastal habitats in Turkey, with the description of a new pan- Mediterranean species of *Echinoderes* (Cyclorhagida: Echinoderidae). Turk. J. Zool. 45, 526–546. https://doi.org/10.3906/zoo-2108-20

Sørensen, M.V., Rho, H.S., Min, W.-G., Kim, D., Chang, C.Y., 2012. An exploration of *Echinoderes* (Kinorhyncha: Cyclorhagida) in Korean and neighboring waters, with the description of four new species and a redescription of *E. tchefouensis* Lou, 1934. Zootaxa 3368, 161–196. https://doi.org/10.11646/zootaxa.3368.1.8

Tanabe, A.S., 2007. KAKUSAN: a computer program to automate the selection of a nucleotide substitution model and the configuration of a mixed model on multilocus data. Mol. Ecol. Notes 7, 962–964. https://doi.org/10.1111/j.1471-8286.2007.01807.x

Veit-Köhler, G., Guilini, K., Peeken, I., Sachs, O., Sauter, E.J., Würzberg, L., 2011. Antarctic deep-sea meiofauna and bacteria react to the deposition of particulate organic matter after a phytoplankton bloom. Deep-Sea Res. II 58, 1983–1995. https://doi.org/10.1016/j.dsr2.2011.05.008

Wessel, P., Smith, W.H.F., Scharroo, R., Luis, J., Wobbe, F., 2013. Generic mapping tools: improved version released. Eos 94, 409–410. https://doi.org/10.1002/2013EO450001

Winnepenninckx, B., Backeljau, T., Mackey, L.Y., Brooks, J.M., De Wachter, R., Kumar, S., Garey, J.R., 1995. 18S rRNA data indicate that Aschelminthes are polyphyletic in origin and consist of at least three distinct clades. Mol. Biol. Evol. 12, 1132– 1137. https://doi.org/10.1093/oxfordjournals.molbev.a040287

Yamaguchi, S., Endo, K., 2003. Molecular phylogeny of Ostracoda (Crustacea) inferred from 18S ribosomal DNA sequences: implication for its origin and diversification. Mar. Biol. 143, 23–38. https://doi.org/10.1007/s00227-003-1062-3

Yamasaki, H., 2015. Two new species of *Dracoderes* (Kinorhyncha: Dracoderidae) from the Ryukyu Islands, Japan, with a molecular phylogeny of the genus. Zootaxa 3980, 359–378. https://doi.org/10.11646/zootaxa.3980.3.2

Yamasaki, H., 2016. *Ryuguderes iejimaensis*, a new genus and species of Campyloderidae (Xenosomata: Cyclorhagida: Kinorhyncha) from a submarine cave in the Ryukyu Islands, Japan. Zool. Anz. 265, 69–79. https://doi.org/10.1016/j.jcz.2016.02.003

Yamasaki, H., Fujimoto, S., 2014. Two new species in the *Echinoderes coulli* group (Echinoderidae, Cyclorhagida, Kinorhyncha) from the Ryukyu Islands, Japan. Zookeys 382, 27–52. http://dx.doi.org/10.3897/zookeys.382.6761

Yamasaki, H., Fujimoto, S., Tanaka, H., 2020a. Three new meiobenthic species from a submarine cave in Japan: *Echinoderes gama*, *E. kajiharai* and *E. uozumii* (Kinorhyncha: Cyclorhagida). J. Mar. Biol. Assoc. U. K. 100, 537–558. https://doi.org/10.1017/S0025315420000429

Yamasaki, H., Herranz, M., Sørensen, M.V., 2020b. An interactive identification key to species of Echinoderidae (Kinorhyncha). Zool. Anz. 287, 14–16. https://doi.org/10.1016/j.jcz.2020.05.002

Yamasaki, H., Hiruta, S.F., Kajihara, H., 2013. Molecular phylogeny of kinorhynchs. Mol. Phylogenet. Evol. 67, 303–310. https://doi.org/10.1016/j.ympev.2013.02.016

Yamasaki, H., Hiruta, S.F., Kajihara, H., Dick, M.H., 2014. Two kinorhynch species (Cyclorhagida, Echinoderidae, *Echinoderes*) show different distribution patterns across Tsugaru Strait, northern Japan. Zool. Sci. 31, 421–429. https://doi.org/10.2108/zs140011

Yamasaki, H., Neuhaus, B., George, K.H., 2019. Echinoderid mud dragons (Cyclorhagida: Kinorhyncha) from Senghor Seamount (NE Atlantic Ocean) including general discussion of faunistic characters and distribution patterns of seamount kinorhynchs. Zool. Anz. 282, 64–87. https://doi.org/10.1016/j.jcz.2019.05.018

Yıldız, N.Ö., Sørensen, M.V., Karaytuğ, S., 2017. A new species of *Cephalorhyncha* Adrianov, 1999 (Kinorhyncha: Cyclorhagida) from the Aegean Coast of Turkey. Helgol. Mar. Res. 70, 24. https://doi.org/10.1186/s10152-016-0476-5

Yoder, M., Tandingan De Ley, I., King, I.W., Mundo-Ocampo, M., Mann, J., Blaxter, M., Poiras, L., De Ley, P., 2006. DESS: a versatile solution for preserving morphology and extractable DNA of nematodes. Nematol. 8, 367–376. https://doi.org/10.1163/156854106778493448

Zelinka, C., 1896. Demonstration der Tafeln der *Echinoderes*-Monographie. Verh. Dtsch. Zool. Ges. 6, 197–199.

Zelinka, C., 1913. Die Echinoderen der Deutschen Südpolar-Expedition 1901–1903. Deutsche Südpolar-Expedition XIV, Zoologie VI, 419–437.

## Figure captions

**Figure 1.** Map of Antarctica indicating the type localities of *P. martinezi* and the sampling stations of *P. shiraseae* in Lützow-Holm Bay, off Cape Darnley, and off Totten Glacier.

**Figure 2.** *Polacanthoderes martinezi*, camera lucida drawings. A, B, holotype female (ZMB 11237), segments 1–11, dorsal view (A) and ventral view (B); C, D, allotype male (ZMB 11238a), segments 10 and 11, dorsal view (C) and ventral view (D). Abbreviations: (ac), acicular spine; gco1/2, type-1/2 glandular cell outlet; LA, lateral accessory; LD, laterodorsal; ltas, lateral terminal accessory spine; lts, lateral terminal spine; LV, lateroventral; MD, middorsal; mdp, middorsal placid; ML, midlateral; mvp, midventral placid; pa, papilla; pe, penile spine; (sac), small acicular spine; SD, subdorsal; se, seta; si, sieve plate; ss, sensory spots; (tu), tube; VL, ventrolateral; VM, ventromedial. Digits in the abbreviations (except for gco1/2) indicate the corresponding segment number.

**Figure 3.** *Polacanthoderes martinezi*, DIC photomicrographs. A, B, D, E, the holotypic female (ZMB 11237), head, neck, and segments 1–5, dorsal view (A) and ventral view (B), segments 6–11, dorsal view (D) and ventral view (E); C, the allotype male (ZMB 11238a), neck and segments 1–6, dorsal view; F, paratype male (ZMB 11238d), segments 7–11, ventral view. Black arrows, white arrowheads, and black arrowheads indicate sensory spot, type-1 glandular cell outlet, and type-2 glandular cell outlet, respectively. Abbreviations: (ac), acicular spine; LA, lateral accessory; LD, laterodorsal; LV, lateroventral; MD, middorsal; ML, midlateral; pa, papilla; pe, penile spine; (sac), small acicular spine; SD, subdorsal; (tu), tube; VL, ventrolateral; VM, ventromedial. Digits in the abbreviations indicate the corresponding segment number.

**Figure 4.** *Polacanthoderes martinezi*, scanning electron micrographs of females. A, segments 2–5, lateroventral view; B, segments 5–7, lateral view; C, segments 6–8, lateroventral view; D, segment 7, lateroventral view. Black arrows and a black arrowhead indicate sensory spot and type-2 glandular cell outlet, respectively. Abbreviations: (ac), acicular spine; LA, lateral accessory; LD, laterodorsal; LV, lateroventral; ML, midlateral; pa, papilla; (sac), small acicular spine; SD, subdorsal; (tu), tube; VM, ventromedial; VL, ventrolateral. Digits in abbreviations indicate the corresponding segment number.

**Figure 5.** *Polacanthoderes shiraseae* sp. nov., camera lucida drawings. A, B, holotype female (ICHUM 8348), segments 1–11, dorsal view (A) and ventral view (B); C, D, paratype male (ICHUM 8371), segments 10 and 11, dorsal view (C) and ventral view (D). Abbreviations: (ac), acicular spine; gco1/2, type-1/2 glandular cell outlet; LA, lateral accessory; LD, laterodorsal; ltas, lateral terminal accessory spine; lts, lateral terminal spine; LV, lateroventral; MD, middorsal; mdp, middorsal placid; ML, midlateral; mvp, midventral placid; pa, papilla; pe, penile spine; (sac), small acicular spine; SD, subdorsal; se, seta; si, sieve plate; SL, sublateral; ss, sensory spots; (tu), tube; VL, ventrolateral; VM, ventromedial. Digits in the abbreviations (except for gco1/2) indicate the corresponding segment number.

**Figure 6.** *Polacanthoderes shiraseae* sp. nov., DIC photomicrographs. A–F, the holotypic female (ICHUM 8348), neck and segments 1–6, dorsal view (A) and ventral view (B), segments 7–11, dorsal view (C) and ventral view (D), segments 6 and 7, ventral view, focused at cuticle surface (E) and focused at deeper layer (F); G and H, paratype male (ICHUM 8371), segments 6–8, ventral view (G), segments 10 and 11, dorsal view (H). Black arrows, white arrowheads, and black arrowheads indicate sensory spot, type-1 glandular cell outlet, and type-2 glandular cell outlet, respectively. Abbreviations: (ac), acicular spine; LA, lateral accessory; LD, laterodorsal; ltas, lateral terminal accessory spine; lts, lateral terminal spine; LV, lateroventral; MD, middorsal; ML, midlateral; pa, papilla; pe, penile spine; (sac), small acicular spine; SD, subdorsal; si, sieve plate; SL, sublateral; (tu), tube; VL, ventrolateral; VM, ventromedial. Digits in the abbreviations indicate the corresponding segment number.

**Figure 7.** *Polacanthoderes shiraseae* sp. nov., scanning electron micrographs of females (A–E) and a male (F). A, overview from lateroventral side; B, head (right side); C, segments 1–4, lateral view; D, segments 1–5, ventral view; E, segments 4–7, lateral view; F, segments 4–6, laterodorsal view. Black arrows and black arrowhead indicate sensory spot and type-2 glandular cell outlet, respectively. Abbreviations: (ac), acicular spine; LA, lateral accessory; LD, laterodorsal; LV, lateroventral; MD, middorsal; ML, midlateral; oos, outer oral style; phc, pharynx crown; psps, primary spinoscalid; (sac), small acicular spine; SD, subdorsal; sec, sector number; SL, sublateral; sps, spinoscalid followed by the corresponding ring number; (tu), tube; VM, ventromedial. Digits after abbreviations (except for sec and sps) indicate the corresponding segment number.

**Figure 8.** Polar-coordinate diagram of mouth cone, introvert, and placids in *Polacanthoderes shiraseae* sp. nov. Grey area and heavy line arcs show mouth cone and placids, respectively. The table lists the arrangement of styles and scalids by sector.

**Figure 9.** *Polacanthoderes shiraseae* sp. nov., scanning electron micrographs of females (A, C–E) and a male (B and F). A, segments 5–7, ventral view; B, segments 6–8, ventral view; C, segments 7–9, lateral view; D, close-up of sieve plate on segment 9; E, segments 8–11, laterodorsal view; F, segments 9–11, ventral view. Black arrows and black arrowhead indicate sensory spot and type-2 glandular cell outlet, respectively. Abbreviations: (ac), acicular spine; LA, lateral accessory; LD, laterodorsal; ltas, lateral terminal accessory spine; lts lateral terminal spine; LV, lateroventral; MD, middorsal; pa, papilla; pe, penile spine; (sac), small acicular spine; SD, subdorsal; se, seta; si, sieve plate; SL, sublateral; (tu), tube; VL, ventrolateral; VM, ventromedial. Digits after abbreviations indicate the corresponding segment number.

**Figure 10.** Maximum-likelihood tree of Kinorhyncha based on 18S (1353 bp) + 28S (2750 bp) dataset. Numbers near nodes are the maximum-likelihood bootstrap (BS) and Bayesian posterior probability (PP) values, respectively; asterisks indicate the node with the full support values (BS=100% and PP=1.00); BS values lower than 50% indicate as polytomy; PP values lower than 0.95 are indicated by dashes. The scale bar indicates branch length in substitutions per site.

**Table 1.** Data on sampling stations, type status, and catalogue numbers of *Polacanthoderes martinezi* and extraction and the specimens of which exoskeleton was lost during the DNA extraction.

| Species | Locality | Sampling station | Sampling date |
|---|---|---|---|
| *Polacanthoderes martinezi* | north of South Shetland Islands | PS105-2/6 | 14 Feb. 2002 |
| *Polacanthoderes shiraseae* sp. nov. | off Cape Darnley | JARE59-CD | 26 Feb. 2018 |
| | off Totten Glacier | JARE61-15 | 17 Dec. 2019 |
| | | JARE61-17 | 18 Dec. 2019 |
| | | JARE61-18 | 18 Dec. 2019 |
| | | JARE61-X23 | 19 Dec. 2019 |
| | Lützow-Holm Bay | JARE61-25 | 19 Dec. 2019 |
| | | JARE61-26 | 19 Dec. 2019 |
| | | JARE61-108 | 05 Mar. 2020 |
| | | JARE61-109 | 05 Mar. 2020 |
| | | JARE61-LH2a | 31 Jan. 2020 |
| | | JARE61-LH3a | 31 Jan. 2020 |
| | | JARE61-LH5a | 30 Jan. 2020 |

*P. shiraseae* sp. nov. "(ex)" and "lost" in the mc

| Depth (m) | Latitude | Longitude | Mounting |
|---|---|---|---|
| 2290 | 61°23′44"S | 58°50′16"W | LM |
| | | | LM |
| | | | SEM |
| 205 | 67°40′38"S | 68°55′22"E | LM |
| | | | LM (ex) |
| | | | lost |
| | | | SEM |
| 691 | 66°47′31"S | 117°21′20"E | LM |
| | | | SEM |
| 608 | 66°45′44"S | 117°44′28"E | LM |
| | | | LM (ex) |
| 523 | 66°45′31"S | 118° 3′38"E | LM |
| | | | SEM |
| 487 | 66°13′43"S | 119°59′17"E | LM |
| | | | LM |
| | | | LM (ex) |
| 627 | 66°37′26"S | 119°20′26"E | LM |
| 693 | 66°29′44"S | 119°33′41"E | LM |
| 309 | 66°29′23"S | 120°47′4"E | LM |
| 431 | 66°22′53"S | 120°40′7"E | LM |
| 310 | 68°42′10"S | 38°30′58"E | LM |
| 264 | 68°28′20"S | 38°29′1"E | LM |
| 219 | 68°51′57"S | 38°53′26"E | LM |
| | | | LM (ex) |
| | | | lost |
| | | | SEM |

ounting column indicate the specimens of which exoskeleton was mounted after DNA

| Type status and catalogue number |
|---|
| 1♀, holotype (ZMB 11237) |
| 2♂, 4♀, paratypes (ZMB 11238a-f) |
| 1♂, 3♀, nontypes (ZMB 11238g-n) |
| 1♂, 3♀, paratypes (ICHUM 8349–8352) |
| 5♂, 6♀, paratypes (ICHUM 8386–8396) |
| 2 individuals |
| 4♂, 1♀, nontypes |
| 2♂, 2♀, paratypes (ICHUM 8353–8356); 1♂, 1♀, paratypes (NHMD 1174924, 1174925) |
| 1♂, 4♀, nontypes |
| 2♂, paratypes (ICHUM 8357–8358) |
| 1♂, paratype (ICHUM 8404) |
| 1♂, 2♀, paratypes (ICHUM 8359–8361); 1♂, 1♀, paratypes (NHMD 1174926, 1174927) |
| 2♂, 1♀, nontypes |
| 1♀, holotype (ICHUM 8348) |
| 2♂, 4♀, paratypes (ICHUM 8362–8367); 1♂, 1♀, paratypes (NHMD 1174928, 1174929) |
| 2♂, 2♀, paratypes (ICHUM 8397–8400) |
| 2♂, 1♀, paratypes (ICHUM 8368–8370) |
| 1♂, paratype (ICHUM 8371) |
| 4♀, paratypes (ICHUM 8372–8375) |
| 2♂, paratypes (ICHUM 8376–8377); 1♂, 1♀, paratypes (NHMD 1174930, 1174931) |
| 1♂, 3♀, paratypes (ICHUM 8378–8381) |
| 1♂, paratype (ICHUM 8382) |
| 2♂, 1♀, paratypes (ICHUM 8383–8385); 1♂, 1♀, paratypes (NHMD 1174932, 1174933) |
| 3♀, paratypes (ICHUM 8401–8403) |
| 2 individuals |
| 2♂, 2♀, nontypes |

**Table 2.** List of PCR and cycle sequencing (CS) primers used in this s

| Gene | Primer name | Reaction PCR |
|---|---|---|
| 18S rRNA (18S) | F1 | PCR & CS |
| | R9 | PCR & CS |
| | F2 | CS |
| | F3 | CS |
| | F4 | CS |
| | R6 | CS |
| | R7 | CS |
| | R8 | CS |
| 28S rRNA (28S) | 28S-01 | PCR & CS |
| | 28Sr | PCR & CS |
| | 28Sf | PCR & CS |
| | 28S-3KR | PCR & CS |
| | 28S-2KF | PCR & CS |
| | 28jj-3´ | PCR & CS |
| | 28S-n05R | CS |
| | 28SR-01 | CS |
| | 28S-15R | CS |
| | 28S-3KF | CS |
| | 28v-5´ | CS |
| | 28S-42F | CS |
| cytochrome *c* oxidase subunit 1 (COI) | LCO | PCR & CS |
| | HCO | PCR & CS |
| | Ki_COIF | PCR & CS |
| | Ki_COIR | PCR & CS |
| | Ec_COIF | PCR & CS |
| | Ec_COIR | PCR & CS |
| | Ec_COIpF | CS |

tudy.

| Primer sequence (in 5′–3′ direction) | Direction | Source |
|---|---|---|
| TACCTGGTTGATCCTGCCAG | Forward | Yamaguchi and Endo (2003) |
| GATCCTTCCGCAGGTTCACCTAC | Reverse | Yamaguchi and Endo (2003) |
| CCTGAGAAACGGCTRCCACAT | Forward | Yamaguchi and Endo (2003) |
| GYGRTCAGATACCRCCSTAGTT | Forward | Yamaguchi and Endo (2003) |
| GGTCTGTGATGCCCTYAGATGT | Forward | Yamaguchi and Endo (2003) |
| TYTCTCRKGCTBCCTCTCC | Reverse | Yamaguchi and Endo (2003) |
| GYYARAACTAGGGCGGTATCTG | Reverse | Yamaguchi and Endo (2003) |
| ACATCTRAGGGCATCACAGACC | Reverse | Yamaguchi and Endo (2003) |
| GACTACCCCCTGAATTTAAGCAT | Forward | Kim et al. (2000) |
| ACACACTCCTTAGCGGA | Reverse | Luan et al. (2005) |
| TGGGACCCGAAAGATGGTG | Forward | Luan et al. (2005) |
| CCAATCCTTTTCCCGAAGTT | Reverse | Yamasaki et al. (2013) |
| TTGGAATCCGCTAAGGAGTG | Forward | Yamasaki et al. (2013) |
| AGTAGGGTAAAACTAACCT | Reverse | Palumbi (1996) |
| CTCACGGTACTTGTTCGCTAT | Reverse | Yamasaki et al. (2013) |
| GACTCCTTGGTCCGTGTTTCAAG | Reverse | Kim et al. (2000) |
| CGATTAGTCTTTCGCCCCTA | Reverse | Yamasaki et al. (2013) |
| AGGTGAACAGCCTCTAGTCG | Forward | Yamasaki et al. (2013) |
| AAGGTAGCCAAATGCCTCATC | Forward | Palumbi (1996) |
| GAGTTTGACTGGGGCGGTA | Forward | Yamasaki et al. (2013) |
| GGTCAACAAATCATAAAGATATTGG | Forward | Folmer et al. (1994) |
| TAAACTTCAGGGTGACCAAAAAATCA | Reverse | Folmer et al. (1994) |
| GGACTGCTTATAGGGTTATTATTCG | Forward | Sánchez et al. (2016) |
| CCCCCTCCTCTAACCTCATAAAA | Reverse | Sánchez et al. (2016) |
| GGGTTTTGATCTCGTCGTTG | Forward | This study |
| CGATGCCATAAATGAAATACATC | Reverse | This study |
| TTTTAATTTTACCTGGGTTTGG | Forward | This study |

**Table 3.** List of taxa included in the phylogenetic analyses.

| Class | Order | Family | Genus and species | Accession n |
|---|---|---|---|---|
| | | | | 18S rRNA |
| Allomalorhagida | Anomoirhaga | Dracoderidae | *Dracoderes abei* | AB738350 |
| | | | *Dracoderes nidhug* | LC007040 |
| | | | *Dracoderes snufkini* | LC032113 |
| | | Franciscideridae | *Gracilideres mawatarii* | AB738378 |
| | | Neocentrophyidae | *Paracentrophyes anurus* | AB738368 |
| | | | *Paracentrophyes quadridentatus* | LC007051 |
| | *incertae sedis* | Pycnophyidae | *Cristaphyes yushini* | AB738370 |
| | | | *Fujuriphyes ponticus* | LC081128 |
| | | | *Fujuriphyes rugosus* | LC081127 |
| | | | *Pycnophyes oshoroensis* | AB738372 |
| | | | *Pycnophyes robustus* | LC007053 |
| | | | *Pycnophyes tubuliferus* | LC081130 |
| | | | *Pycnophyes zelinkaei* | LC007055 |
| | | | *Setaphyes dentatus* | LC007052 |
| | | | *Setaphyes flaveolatus* | LC081129 |
| Cyclorhagida | Echinorhagata | Echinoderidae | *Cephalorhyncha* sp. | AB738352 |
| | | | *Echinoderes dujardinii* | LC007044 |
| | | | *Echinoderes hwiizaa* | AB899167 |
| | | | *Echinoderes komatsui* | AB899164 |
| | | | *Echinoderes microaperturus* | LC007046 |
| | | | *Echinoderes ohtsukai* | LC096961 |
| | | | *Echinoderes rex* | LC081126 |
| | | | *Echinoderes sensibilis* | LC007047 |
| | | | *Meristoderes macracanthus* | LC007049 |
| | | | *Meristoderes* sp. | LC007050 |
| | | | *Polacanthoderes shiraseae* sp. nov. | LC721243 |
| | Kentrorhagata | Centroderidae | *Centroderes* sp. | LC008445 |
| | | | *Condyloderes* sp. 1 | LC007038 |
| | | | *Condyloderes* sp. 2 | LC007039 |
| | | Semnoderidae | *Antygomonas* sp. 1 | AB738340 |
| | | | *Antygomonas* sp. 2 | AB738342 |
| | | | *Semnoderes armiger* (Italian population) | LC007056 |
| | | | *Semnoderes armiger* (Norwegian population) | LC007057 |
| | | | *Sphenoderes poseidon* | AB738364 |
| | | Zelinkaderidae | *Triodontoderes anulap* | LC007058 |
| | | | *Zelinkaderes sp.* | AB738366 |
| | | *incertae sedis* | *Tubulideres seminoli* | LC007059 |
| | Xenosomata | Campyloderidae | *Campyloderes* sp. 1 | AB738344 |
| | | | *Campyloderes* sp. 2 | AB738346 |
| OUTGROUP (Priapulida) | | | *Priapulus caudatus* | X87984 |
| OUTGROUP (Nematoda) | | | *Xiphinema rivesi* | HM921344 |

| umber<br>28S rRNA | Reference |
|---|---|
| AB738351 | Yamasaki et al. (2013) |
| LC007064 | Sørensen et al. (2015) |
| LC032114 | Yamasaki (2015) |
| AB738378 | Yamasaki et al. (2013) |
| AB738368 | Yamasaki et al. (2013) |
| LC007076–77 | Sørensen et al. (2015) |
| AB738371 | Yamasaki et al. (2013) |
| LC081133 | Sánchez et al. (2016) |
| LC081132 | Sánchez et al. (2016) |
| AB738373 | Yamasaki et al. (2013) |
| LC007070 | Sørensen et al. (2015) |
| LC081135 | Sánchez et al. (2016) |
| LC007071 | Sørensen et al. (2015) |
| LC007069 | Sørensen et al. (2015) |
| LC081134 | Sánchez et al. (2016) |
| AB738353 | Yamasaki et al. (2013) |
| LC007065 | Sørensen et al. (2015) |
| AB899168 | Yamasaki and Fujimoto (2014) |
| AB899165 | Yamasaki and Fujimoto (2014) |
| LC007066 | Sørensen et al. (2015) |
| LC096962 | Randsø et al. (2019) |
| LC081131 | Sánchez et al. (2016) |
| LC032121 | Sørensen et al. (2015); Yamasaki (2015) |
| LC007067 | Sørensen et al. (2015) |
| LC007068 | Sørensen et al. (2015) |
| LC721244 | This study |
| LC008446 | Sørensen et al. (2015) |
| LC007062 | Sørensen et al. (2015) |
| LC007063 | Sørensen et al. (2015) |
| AB738341 | Yamasaki et al. (2013) |
| AB738343 | Yamasaki et al. (2013) |
| LC007072 | Sørensen et al. (2015) |
| LC007073 | Sørensen et al. (2015) |
| AB738365 | Yamasaki et al. (2013) |
| LC007074 | Sørensen et al. (2015) |
| AB738367 | Yamasaki et al. (2013) |
| LC007075 | Sørensen et al. (2015) |
| AB738345 | Yamasaki et al. (2013) |
| AB738347 | Yamasaki et al. (2013) |
| AY210840 | Winnepenninckx et al. (1995); Mallatt et al. (2004) |
| Ay210845 | Gutiérrez-Gutiérrez et al. (2011); Mallatt et al. (2004) |

**Table 4.** Summary of locations of cuticular structures and spines in *Polacanthoderes martine* characters indicate the characters not reported in the original description in Sørensen (2008a). characters were usually absent, but appear in some specimens. Asterisks indicate the characte moved its position. Abbreviations: ac, acicular spine; gco1/2, type-1/2 glandular cell outlet; L accessory; LD, laterodorsal; ltas, lateral terminal accessory spine; lts, lateral terminal spine; L MD, middorsal; ML, midlateral; PD, paradorsal; pe, penile spine; sac, smaller acicular spine; se, seta; si, sieve plate; SL, sublateral; ss, sensory spot; tu, tube; VL, ventrolateral; VM, ventr

| Position segment | MD | PD | SD | LD | ML | SL | LA | LV | VL |
|---|---|---|---|---|---|---|---|---|---|
| 1 | gco1 | | ss | ss | | ss | | | |
| 2 | gco1, ss | | (tu) | ss, ss | | | | | |
| 3 | gco1 | | ss | ss | ss | | | | |
| 4 | ac | gco1 | ss | | tu* | | | | |
| 5 | ac | gco1 | (sac or tu), ss | | sac, ss | | | tu | |
| 6 | ac | gco1, ss | sac, ss | sac | gco2 | | sac | ac | |
| 7 | ac | gco1, ss | sac, ss | sac | ss | | sac | ac | pa (♀) |
| 8 | ac | gco1, ss | (sac), ss | sac* | gco2 | | sac | ac | sac, ss |
| 9 | | gco1 | ss, ss | sac* | | si | sac | ac | sac*, ss |
| 10 | gco1, gco1 | | ss | tu | | | | | sac |
| 11 | gco1, gco1 | | ss | | | | pe×3 (♂), ltas (♀) | lts | |

*zi* . Underlined
. Parenthetic
r rarely absent or
.A, lateral
.V, lateroventral;
SD, subdorsal;
omedial; (♀),

| VM |
|---|
| gco1, ss |
| gco1, ss |
| gco1, ss |
| sac, gco1, ss |
| sac, gco1, ss |
| sac, gco1, pa (♀) |
| sac, gco1, ss |
| gco1 |
| gco1 |
| gco1 |
| se |

**Table 5.** Measurements for adult *Polacanthoderes shiraseae* sp. nov. (in micrometers). Columns N and SD inc size and standard deviation, respectively. Numbers in the Character column indicate the corresponding segmen Abbreviations: (ac), acicular spine; LA, length of lateral accessory character; LD, length of laterodorsal charac of lateral terminal accessory spine; lts, length of lateral terminal spine; LV, length of lateroventral character; M middorsal character; MSW, maximum sternal width; pe, length of penile spine; S, segment length; (sac), small SD, length of subdorsal character; SL, length of sublateral character; SW, standard width; TL, trunk length; (tu length of ventromedial character.

| Character | Holotype | Range | N | Mean | SD | Character | Holotype | Range | N |
|---|---|---|---|---|---|---|---|---|---|
| TL | 453 | 369–512 | 65 | 454.7 | 23.63 | MD6 (ac) | 98 | 90–116 | 65 |
| MSW-7 | 80 | 72–89 | 54 | 80.6 | 4.02 | SD6 (sac) | 20 | 17–28 | 67 |
| MSW/TL | 17.69% | 16.33%–20.30% | 54 | 17.80% | 0.93% | LD6 (sac) | 22 | 16–30 | 67 |
| SW-10 | 68 | 61–73 | 55 | 66.9 | 2.91 | LA6 (sac) | 15 | 12–20 | 67 |
| SW/TL | 14.99% | 13.12%–17.32% | 55 | 14.78% | 0.87% | LV6 (ac) | 28 | 21–30 | 67 |
| S1 | 50 | 48–57 | 62 | 51.9 | 1.87 | VM6 (sac) | 14 | 12–22 | 67 |
| S2 | 32 | 27–42 | 62 | 33.0 | 2.34 | MD7 (ac) | 118 | 104–131 | 61 |
| S3 | 36 | 30–44 | 62 | 36.2 | 2.55 | SD7 (sac) | 20 | 18–29 | 67 |
| S4 | 40 | 33–47 | 62 | 40.0 | 2.75 | LD7 (sac) | 23 | 18–29 | 67 |
| S5 | 40 | 36–47 | 62 | 41.3 | 2.3 | SL7 (sac) | 20 | 16–24 | 67 |
| S6 | 46 | 41–51 | 62 | 45.9 | 2.4 | LV7 (ac) | 31 | 23–32 | 67 |
| S7 | 49 | 44–57 | 62 | 49.6 | 2.47 | VM7 (sac) | 15 | 13–19 | 67 |
| S8 | 57 | 53–62 | 63 | 57.3 | 2.2 | MD8 (ac) | 150 | 131–167 | 63 |
| S9 | 58 | 49–68 | 63 | 57.8 | 3.11 | LD8 (sac) | 20 | 15–26 | 67 |
| S10 | 76 | 65–81 | 63 | 73.7 | 3.69 | LA8 (sac) | 18 | 14–24 | 67 |
| S11 | 48 | 37–52 | 63 | 45.3 | 2.6 | LV8 (ac) | 45 | 40–52 | 67 |
| MD4 (ac) | 61 | 51–71 | 66 | 61.9 | 4.72 | VL8 (sac) | 14 | 13–22 | 67 |
| SD4 (sac) | n.a. | 16–25 | 14 | 22.2 | 2.33 | LD9 (sac) | 23 | 16–26 | 67 |
| LD4 (tu) | 17 | 12–20 | 64 | 16.4 | 1.64 | LA9 (sac) | 17 | 13–22 | 67 |
| VM4 (sac) | 12 | 10–17 | 67 | 12.6 | 1.42 | LV9 (ac) | 41 | 31–51 | 67 |
| MD5 (ac) | 81 | 51–92 | 64 | 79.7 | 6.72 | VL9 (sac) | 14 | 13–22 | 67 |
| SD5 (sac) | n.a. | 18–27 | 18 | 22.4 | 2.38 | LD10 (tu) | 14 | 11–19 | 66 |
| LD5 (sac) | 22 | 14–24 | 67 | 20.7 | 2.08 | VL10 (sac) | 15 | 13–22 | 67 |
| LV5 (tu) | 14 | 12–19 | 67 | 15.5 | 1.67 | lts | 231 | 202–265 | 65 |
| VM5 (sac) | 12 | 11–22 | 67 | 13.7 | 1.76 | lts/TL | 51.10% | 45.01%–60.02% | 63 |
| | | | | | | ltas | 82 | 73–102 | 37 |
| | | | | | | ltas/TL | 18.02% | 15.88%–22.26% | 36 |
| | | | | | | pe | n.a. | 88–106 | 30 |
| | | | | | | pe/TL | n.a. | 18.77%–25.92% | 29 |

licate sample
t.
ter; ltas, length
[D, length of
acicular spine;
), tube; VM,

| Mean | SD |
|---|---|
| 100.6 | 5.85 |
| 23.6 | 2.52 |
| 21.8 | 2.22 |
| 15.8 | 1.69 |
| 25.6 | 2.15 |
| 15.0 | 1.63 |
| 117.1 | 6.39 |
| 24.2 | 2.37 |
| 23.1 | 1.81 |
| 20.9 | 1.7 |
| 28.0 | 2.16 |
| 16.6 | 1.36 |
| 148.2 | 7.27 |
| 21.2 | 1.96 |
| 18.7 | 1.89 |
| 45.0 | 2.92 |
| 16.9 | 1.8 |
| 21.0 | 1.63 |
| 17.3 | 1.64 |
| 40.1 | 3.44 |
| 16.9 | 1.81 |
| 14.7 | 1.91 |
| 16.7 | 2.07 |
| 235.9 | 13.88 |
| 51.95% | 3.57% |
| 85.2 | 6.18 |
| 18.52% | 1.37% |
| 96.1 | 4.66 |
| 21.56% | 1.45% |

**Table 6.** Summary of locations of cuticular structures and spines in *Polacanthoderes shiras*
Parenthetic characters indicate the features usually absent, but found in some specimens. As
character rarely absent in one or both sides, moved to adjacent position, or additional one pr
Abbreviations: ac, acicular spine; gco1/2, type-1/2 glandular cell outlet; LA, lateral accesso
ltas, lateral terminal accessory spine; lts, lateral terminal spine; LV, lateroventral; MD, mid
midlateral; PD, paradorsal; pe, penile spine; sac, smaller acicular spine; SD, subdorsal; se, s
SL, sublateral; ss, sensory spot; tu, tube; VL, ventrolateral; VM, ventromedial; (♀), characte

| Position segment | MD | PD | SD | LD | ML | SL | LA | LV | VL |
|---|---|---|---|---|---|---|---|---|---|
| 1 | gco1 | | ss | ss | | ss | | | |
| 2 | gco1, ss | | | ss, ss | | | | | |
| 3 | gco1 | | ss | ss | ss | | | | |
| 4 | ac | gco1 | (sac), ss | | tu* | | | | |
| 5 | ac | gco1 | (sac), ss | | sac, ss | | | tu | |
| 6 | ac | gco1, ss | sac, ss | sac | gco2 | | sac* | ac | |
| 7 | ac | gco1, ss | sac, ss | sac* | ss | sac* | | ac | pa (♀) |
| 8 | ac | gco1, ss | (sac), ss | sac | gco2, ss | | sac | ac | sac, ss |
| 9 | | gco1 | ss, ss | sac, ss | | si | sac | ac | sac, ss |
| 10 | gco1, gco1 | | ss | tu | | | | | sac, ss |
| 11 | gco1, gco1 | | ss | | | | pe×3 (♂), ltas (♀) | lts | |

*seae* sp. nov.
sterisks indicate the
resent in one side.
ry; LD, laterodorsal;
dorsal; ML,
seta; si, sieve plate;
r found in female;

| VM |
|---|
| gco1, ss |
| gco1, ss |
| gco1, ss |
| sac, gco1, ss |
| sac, gco1, ss |
| sac, gco1, ss, pa (♀) |
| sac, gco1, ss |
| gco1 |
| gco1 |
| gco1 |
| se |

**Table 7.** K2P distances (percent) based on 541 bp of COI sequences within and among the three populations of *Polacanthoderes shiraseae* sp. nov. Parenthetic number after the locality name indicates the number of the sequenced individuals for each population.

| | off Cape Darnley | off Totten Glacier | Lützow-Holm Bay |
|---|---|---|---|
| off Cape Darnley (12) | 0–0.6 | | |
| off Totten Glacier (5) | 0–0.6 | 0–0.4 | |
| Lützow-Holm Bay (4) | 0.6–1.3 | 0.6–1.5 | 0.6–1.5 |

Figure 1

Click here to access/download;Figure;Fig 1 Map.tif

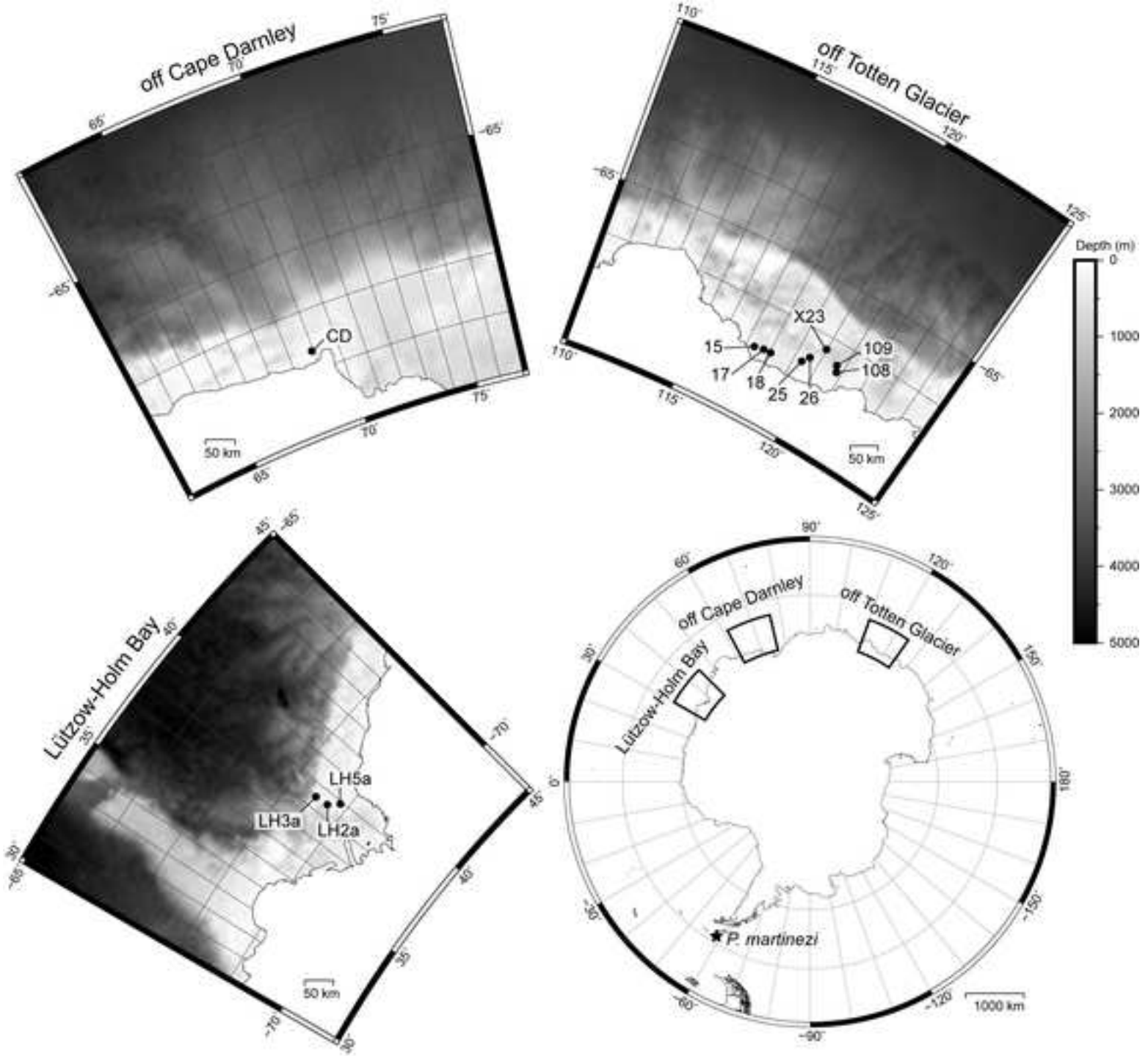

Figure 2

Click here to access/download;Figure;Fig 2 Polacanthoderes martinezi .tif

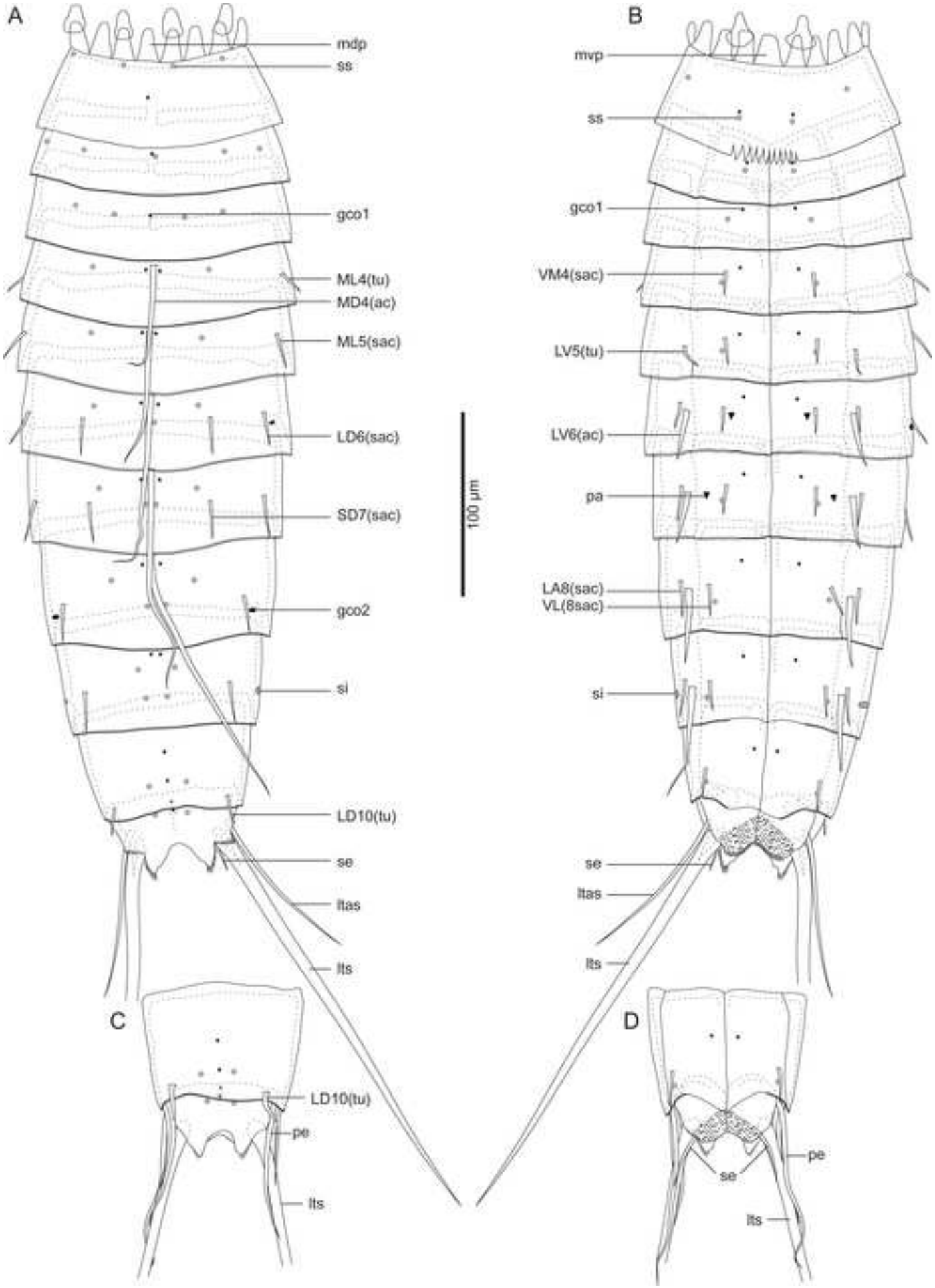

Figure 3

Click here to access/download;Figure;Fig 3 P martinez LM.tif

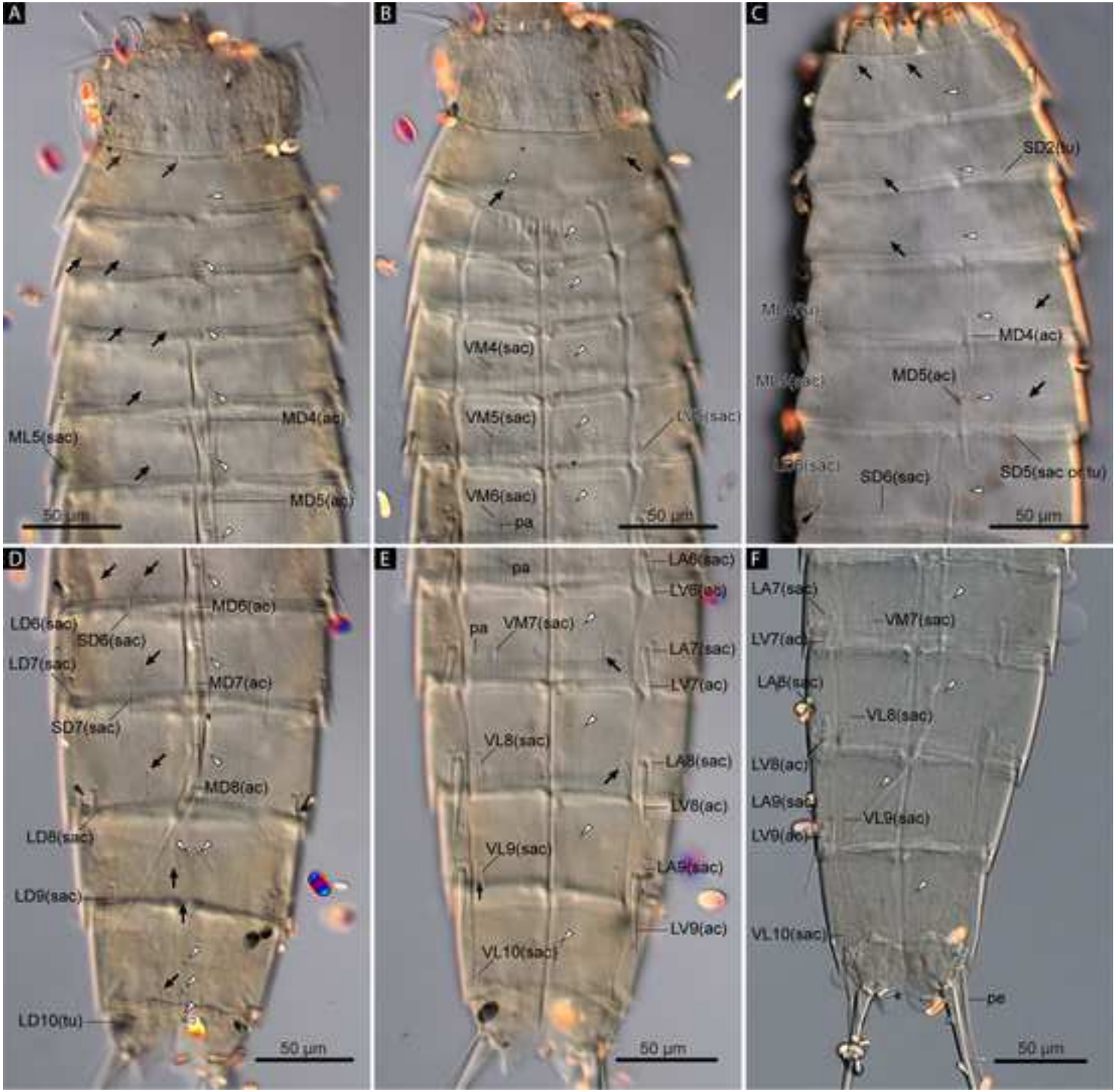

Figure 4

Click here to access/download;Figure;Fig 4 P martinezi SEM.tif

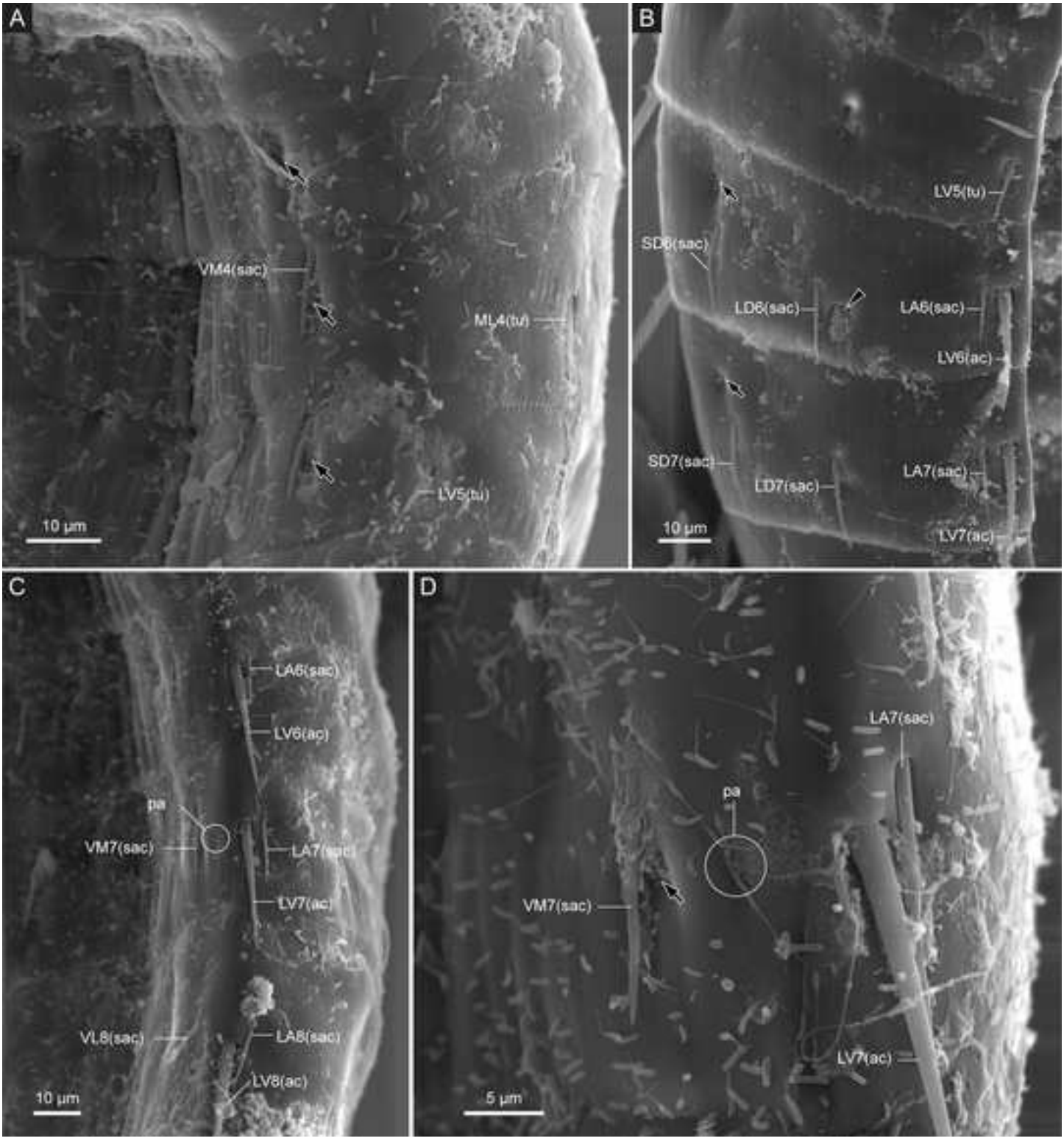

Figure 5

Click here to access/download;Figure;Fig 5 P shiraseae_R1.tif

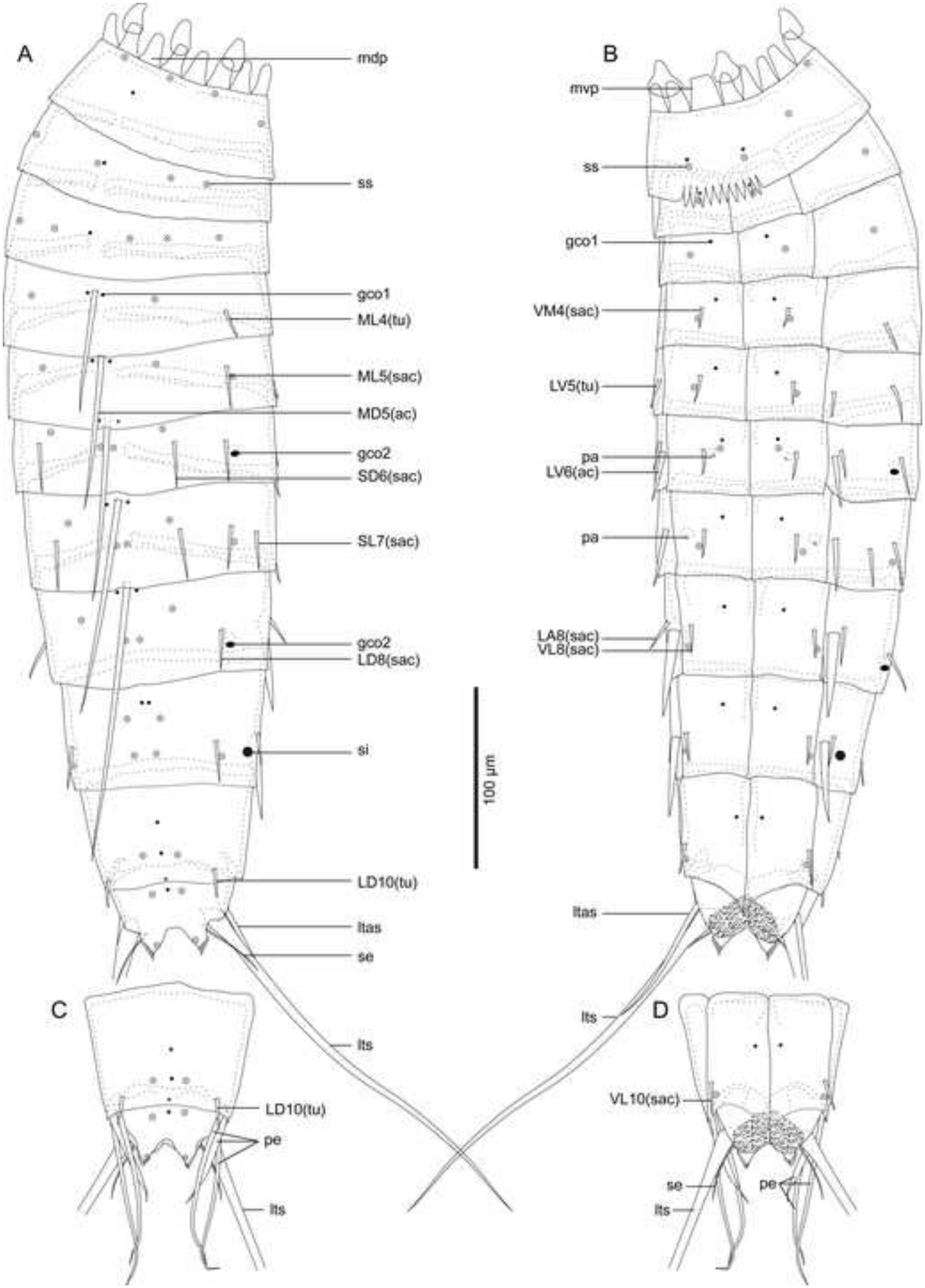

Figure 6

Click here to access/download;Figure;Fig 6 P shiraseae LM_R1.tif

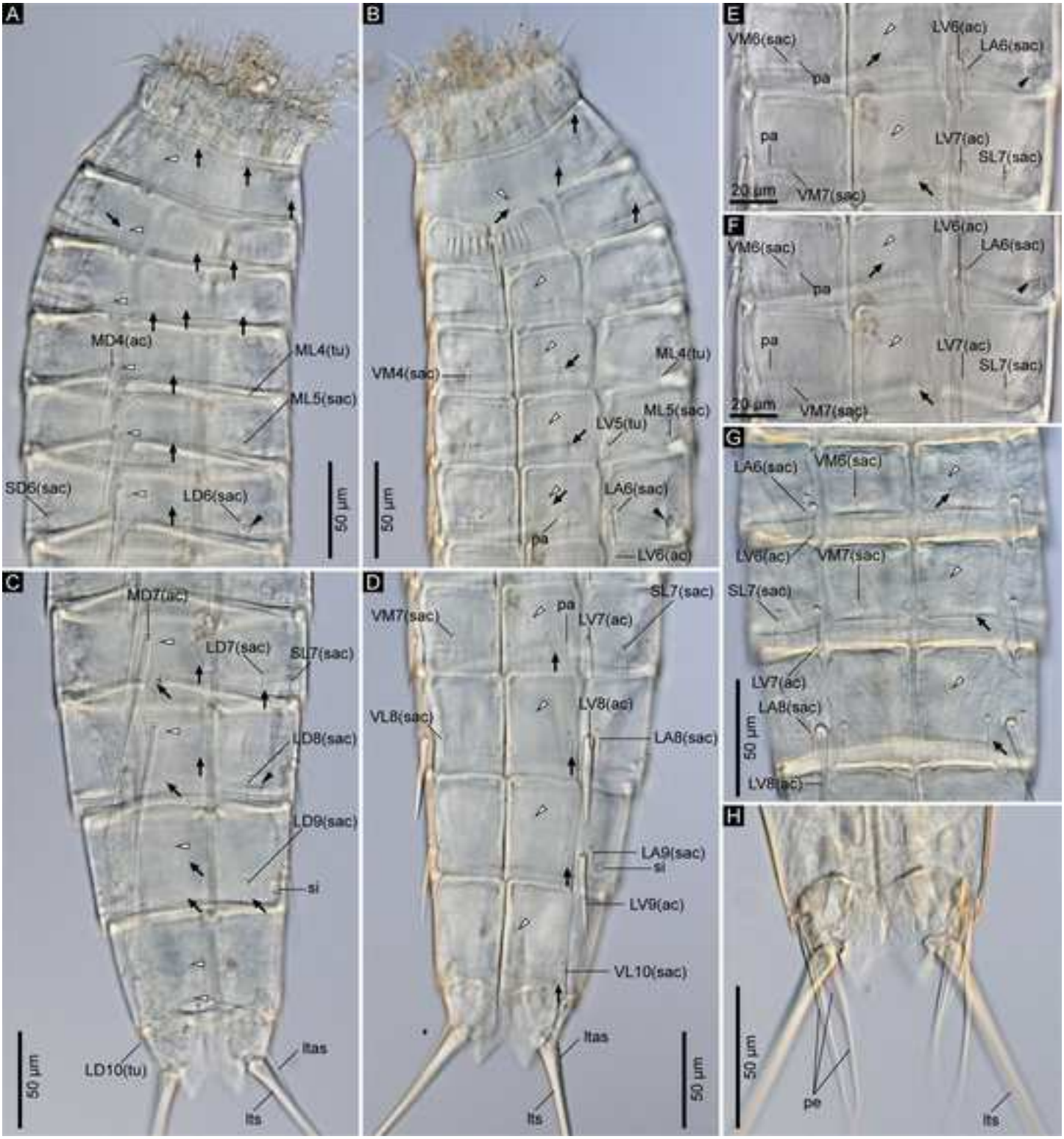

Figure 7

Click here to access/download;Figure;Fig 7 P shiraseae SEM1_R1.tif

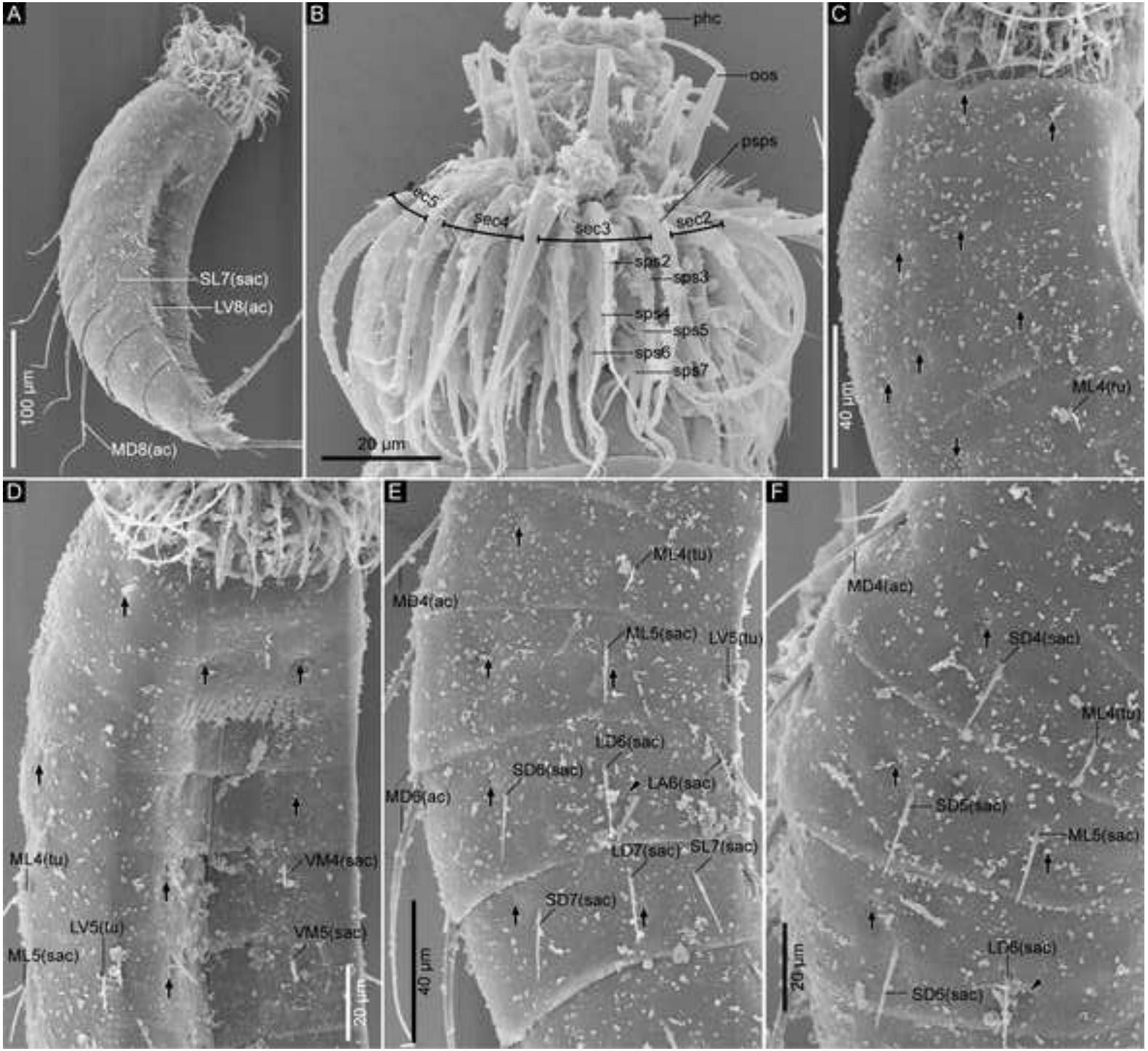

Figure 8



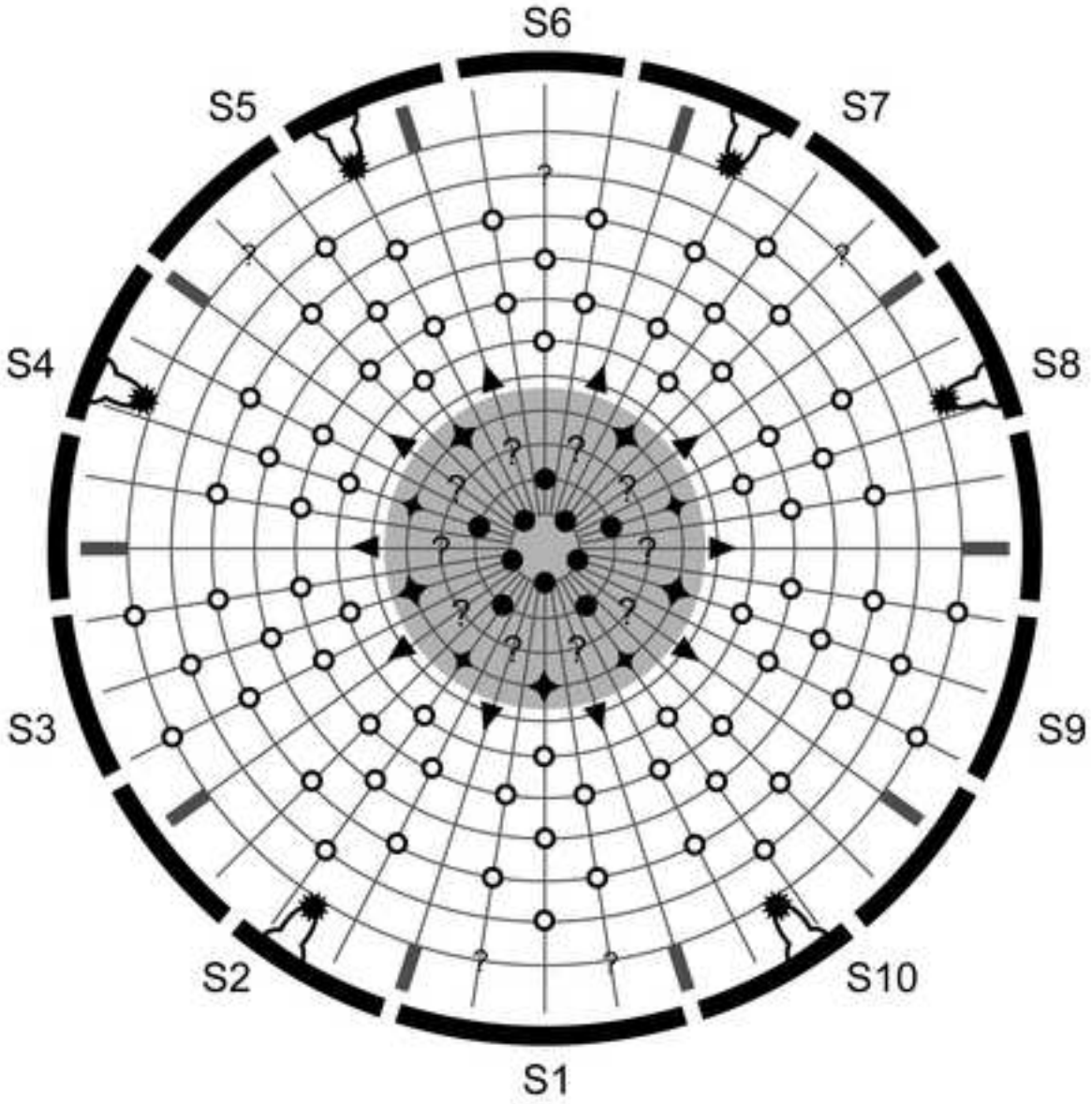


Scalid and style arrangement

| Ring/Section | | 1 | 2 | 3 | 4 | 5 | 6 | 7 | 8 | 9 | 10 | Total |
|---|---|---|---|---|---|---|---|---|---|---|---|---|
| -03 inner oral styles | ● | 1 | 0 | 1 | 0 | 1 | 0 | 1 | 0 | 1 | 0 | 5 |
| -02 inner oral styles | ● | 0 | 1 | 0 | 1 | 0 | 1 | 0 | 1 | 0 | 1 | 5 |
| -01 inner oral styles | ? | ? | ? | ? | ? | ? | ? | ? | ? | ? | ? | ? |
| 00 outer oral styles | ✦ | 1 | 1 | 1 | 1 | 1 | 0 | 1 | 1 | 1 | 1 | 9 |
| 01 primary spinoscalids | ▼ | 1 | 1 | 1 | 1 | 1 | 1 | 1 | 1 | 1 | 1 | 10 |
| 02 spinoscalids | ○ | 1 | 1 | 1 | 1 | 1 | 1 | 1 | 1 | 1 | 1 | 10 |
| 03 spinoscalids | ○ | 2 | 2 | 2 | 2 | 2 | 2 | 2 | 2 | 2 | 2 | 20 |
| 04 spinoscalids | ○ | 1 | 1 | 1 | 1 | 1 | 1 | 1 | 1 | 1 | 1 | 10 |
| 05 spinoscalids | ○ | 2 | 2 | 2 | 2 | 2 | 2 | 2 | 2 | 2 | 2 | 20 |
| 06 spinoscalids | ○ | 1 | 1 | 1 | ? | 1 | ? | 1 | ? | 1 | 1 | ≥7 |
| 07 spinoscalids | ○ | ? | 0 | 2 | 0 | ? | ? | ? | 0 | 2 | 0 | ≥4 |
| trichoscalids | ✸ | 0 | 1 | 0 | 1 | 1 | 0 | 1 | 1 | 0 | 1 | 6 |

Figure 9

Click here to access/download;Figure;Fig 9 P shiraseae SEM2.tif

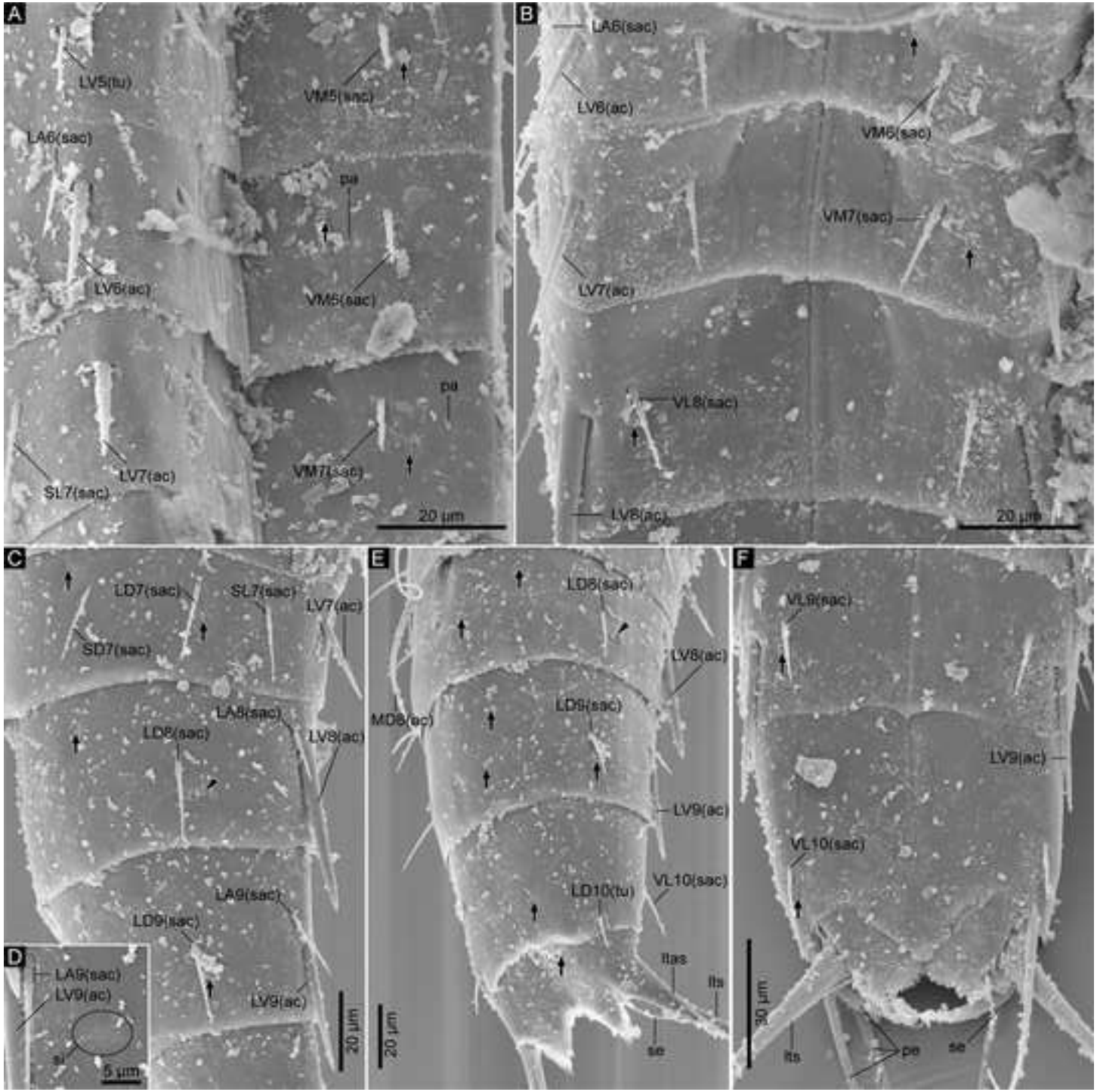

Figure 10

Click here to access/download;Figure;Fig 10 ML_tree_with_BS_PP.tif